Environ Geochem Health
https://doi.org/10.1007/s10653-019-00345-z

ORIGINAL PAPER

Source and background threshold values of potentially toxic elements in soils by multivariate statistics and GIS-based mapping: a high density sampling survey in the Parauapebas basin, Brazilian Amazon

Prafulla Kumar Sahoo · Roberto Dall'Agnol · Gabriel Negreiros Salomão · Jair da Silva Ferreira Junior · Marcio Souza da Silva · Gabriel Caixeta Martins · Pedro Walfir Martin e Souza Filho · Mike A. Powell · Clovis Wagner Maurity · Rômulo Simões Angelica · Marlene Furtado da Costa · José Oswaldo Siqueira

Received: 18 December 2018 / Accepted: 5 June 2019

Abstract A high-density regional-scale soil geochemical survey comprising 727 samples (one sample per each 5 × 5 km grid) was carried out in the Parauapebas sub-basin of the Brazilian Amazonia, under the Itacaiúnas Basin Geochemical Mapping and Background Project. Samples were taken from two depths at each site: surface soil, 0–20 cm and deep soil, 30–50 cm. The ground and sieved (< 75 μm) fraction was digested using aqua regia and analyzed for 51 elements by inductively coupled plasma mass spectrometry (ICPMS). All data were used here, but the principal focus was on the potential toxic elements (PTEs) and Fe and Mn to evaluate the spatial distribution patterns and to establish their geochemical background concentrations in soils. Geochemical maps as well as principal component analysis (PCA) show that the distribution patterns of the elements are very similar between surface and deep soils. The PCA, applied on clr-transformed data, identified four major associations: Fe–Ti–V–Sc–Cu–Cr–Ni (Gp-1); Zr–Hf–U–Nb–Th–Al–P–Mo–Ga (Gp-2); K–Na–Ca–Mg–Ba–

Electronic supplementary material The online version of this article (https://doi.org/10.1007/s10653-019-00345-z) contains supplementary material, which is available to authorized users.

P. K. Sahoo (✉) · R. Dall'Agnol · G. N. Salomão · J. da Silva Ferreira Junior · M. S. da Silva · G. C. Martins · P. W. M. e Souza Filho · C. W. Maurity · J. O. Siqueira
Instituto Tecnológico Vale (ITV), Rua Boaventura da Silva, 955, Belém, PA 66055-090, Brazil
e-mail: prafulla.sahoo@itv.org; prafulla.iitkgp@gmail.com

P. K. Sahoo
Department of Environmental Science and Technology, School of Environmental and Earth Sciences, Central University of Punjab, Bathinda 151001, India

R. Dall'Agnol · G. N. Salomão · P. W. M. e Souza Filho · C. W. Maurity · R. S. Angelica
Programa de Pós-graduação em Geologia e Geoquímica, Instituto de Geociências (IG), Universidade Federal do Pará (UFPA), Rua Augusto Corrêa, Belém, PA 66075-110, Brazil

M. S. da Silva
Programa de Pós-graduação em Ciências Ambientais, Instituto de Geociências (IG), Universidade Federal do Pará (UFPA), Rua Augusto Corrêa, Belém, PA 66075-110, Brazil

M. A. Powell
Department of Renewable Resources, Faculty of Agriculture, Life and Environmental Sciences (ALES), University of Alberta, Edmonton, Canada

M. F. da Costa
Gerência de Meio Ambiente - Minas de Carajás, Departamento de Ferrosos Norte, Estrada Raymundo Mascarenhas, S/N Mina de N4, Parauapebas, PA 68516-000, Brazil

Published online: 10 August 2019

Rb–Sr (Gp-3); and La–Ce–Co–Mn–Y–Zn–Cd (Gp-4). Moreover, the distribution patterns of elements varied significantly among the three major geological domains. The whole data indicate a strong imprint of local geological setting in the geochemical associations and point to a dominant geogenic origin for the analyzed elements. Copper and Fe in Gp-1 were enriched in the Carajás basin and are associated with metavolcanic rocks and banded-iron formations, respectively. However, the spatial distribution of Cu is also highly influenced by two hydrothermal mineralized copper belts. Ni–Cr in Gp-1 are highly correlated and spatially associated with mafic and ultramafic units. The Gp-2 is partially composed of high field strength elements (Zr, Hf, Nb, U, Th) that could be linked to occurrences of A-type Neoarchean granites. The Gp-3 elements are mobile elements which are commonly found in feldspars and other rock-forming minerals being liberated by chemical weathering. The background threshold values (BTV) were estimated separately for surface and deep soils using different methods. The '75th percentile', which commonly used for the estimation of the quality reference values (QRVs) following the Brazilian regulation, gave more restrictive or conservative (low) BTVs, while the 'M_{MAD}' was more realistic to define high BTVs that can better represent the so-called mineralized/normal background. Compared with CONAMA Resolution (No. 420/2009), the conservative BTVs of most of the toxic elements were below the prevention limits (PV), except Cu, but when the high BTVs are considered, Cu, Co, Cr and Ni exceeded the PV limits. The degree of contamination (C_{deg}), based on the conservative BTVs, indicates low contamination, except in the Carajás basin, which shows many anomalies and had high contamination mainly from Cu, Cr and Ni, but this is similar between surface and deep soils indicating that the observed high anomalies are strictly related to geogenic control. This is supported when the C_{deg} is calculated using the high BTVs, which indicates low contamination. This suggests that the use of only conservative BTVs for the entire region might overestimate the significance of anthropogenic contamination; thus, we suggest the use of high BTVs for effective assessment of soil contamination in this region. The methodology and results of this study may help developing strategies for geochemical mapping in other Carajás soils or in other Amazonian soils with similar characteristics.

Keywords Soil geochemical mapping · Potentially toxic elements · Geochemical background · Environmental contamination · Multivariate analysis · Southeastern Amazon

Introduction

Soil is considered one of the most important and complicated biogeochemical systems; metals in soils impact surface and subsurface waters, enter the food chain via plants and animals, and ultimately impact ecosystem functioning and quality of human life (Jiao et al. 2015; Pandolfo et al. 2008; Teh et al. 2016). Soil is both a source and sink of elements, including the potentially toxic elements (PTEs) such as As, Ba, Cd, Co, Cr, Cu, Hg, Mo, Mn, Fe, Ni, Pb, Sn, V, and Zn. Their natural spatial distribution levels vary significantly in soils depending on the heterogeneity of parent rocks, local mineralization, and soil-forming factors (e.g., weathering, climate, topography, vegetation, and time (Kabata-Pendias and Mukherjee 2007; Martinez-Lladó et al. 2008; Palumbo et al. 2000; Towett et al. 2015). Geochemical sorption with clays, Fe-oxyhydroxides and/or organic matter, and/or mineral diagenesis can influence the occurrence and distribution of metals in soils. Even though the nature of the parent materials has an important influence on the total elemental deportment in the soil systems (Towett et al. 2015), anthropogenic activities, such as mining, smelting, agriculture, industrial and waste disposal, may have a much greater influence on occurrence and distribution of metals (Wang et al. 2018). For this reason, it is important to determine background concentrations of PTEs in soils and identify their origin with respect to natural (geogenic) and anthropogenic sources in order to manage soils quality and reduce exposure risk from the long-term accumulation of heavy metals (Kabata-Pendias and Mukherjee 2007; Towett et al. 2015).

Mapping the spatial distribution of soil elements is a useful tool for identifying potential sources and/or linking their occurrence to geological/geochemical

factors (Lancianese and Dinelli 2015; Reimann and de Caritat 2017; Salomão et al. 2018; Xie et al. 2008). This information can be used to inform the decision-making process during land management (De Vivo et al. 2003, 2004; Thornton et al. 2008). When constructing geochemical maps, some important criteria should be considered; high-density sampling is one of the key points as it increases exponentially with the amount of information required (Chiprés et al. 2008; Lancianese and Dinelli 2015; Ohta et al. 2011; Xie et al. 2008). This technique can be very important for determining the impact of various anthropogenic activities, as well as relationships with bedrock geology/specific mineralogy (Lancianese and Dinelli 2015; Salomão et al. 2018; Yamamoto et al. 2007). Ultimately, this technique may be more suitable for describing background values and delineating site-specific geochemical anomalies (Salomão et al. 2018; Maritz et al. 2010). In addition, multivariate analysis such as principal component analysis (PCA) is crucial at regional to local scales for clustering soil characteristics related to parent rock and/or soil-forming factors (Kabata-Pendias and Mukherjee 2007; Wang et al. 2018; Zuo 2011). In this context, the complex spatial variations of elements, and their pathways, can be better understood by combining multivariate analysis with geochemical mapping (Wang et al. 2018). Furthermore, knowing vertical elemental distribution can help identity the anthropogenic impact on surface versus deep soils and the relative importance of anthropogenic versus natural influences (Deschenes et al. 2013). This, in turn, could help in finding potential contaminated sites.

Determining the level of soil contamination is typically based on comparison with reference values or guideline values as defined in legal regulations and guidelines (Paye et al. 2010). In Brazil, soil environmental guidelines are defined in Resolution No. 420/2009 of the Brazilian Council for the Environment and are defined as quality references values (QRV); prevention values (PV); and investigation values (IV) (CONAMA 2009). However, taking into account the Brazilian territorial extent and soil heterogeneity depending on local geomorphology, pedology, and lithology, the elemental concentrations vary significantly from one place to another. For this reason, it is essential to define site-specific regional background levels for metals to set up limits for distinction between natural concentrations and those derived from anthropogenic contamination, which is fundamental to the management of soil quality and risk assessment (Reimann et al. 2018; Reimann and Garrett 2005; Galuszka 2007). This type of work is also important for informing policy at all government levels related as developing guidelines/legislation to control the risk associated with metal contaminations in soils (Morton-Bermea et al. 2009; Salminen and Tarvainen 1997). Several standard methods have been developed for the estimation of background values in soils depending on the data distributions, number of samples, and purposes (Ander et al. 2013; Marandi and Karro 2008; Matschullat et al. 2000; Nakic et al. 2007; Reimann et al. 2005, 2018).

Given the lack of specific regional geochemical background values in soils in several locations in Brazil, in particular Amazonia, this paper aims to establish background threshold values (BTV) for the Parauapebas river sub-basin under the Itacaiúnas Geochemical Mapping and Background Project (ItacGMBP), being executed at the Institute Tecnológico Vale. It should be noted that the municipalities of Parauapebas and Canaã dos Carajás are located in the Carajás Mining Complex in southeast Pará state of Brazil (Fig. 1) which has experienced a significant change in the land use to foster economic and social development through mining, urbanization, construction of roads and railways, and expansion of cattle farming (Souza-Filho et al. 2016). These changes have led to serious environmental concerns related to soil health, which further highlight the crucial need for establishing metal background values in the Parauapebas basin. The main objectives of this study were: (1) to evaluate the source and spatial distribution of elements, especially for PTEs, and to define their lithogenic or anthropogenic origin using geochemical mapping and multivariate statistics; (2) to determine their geochemical background concentrations in soils; and (3) to evaluate the extent of heavy metal contamination in soils by comparison with contamination indices and the maximum limits recommended in Brazilian legislation. The results of this study may help with soil quality management in this region, as

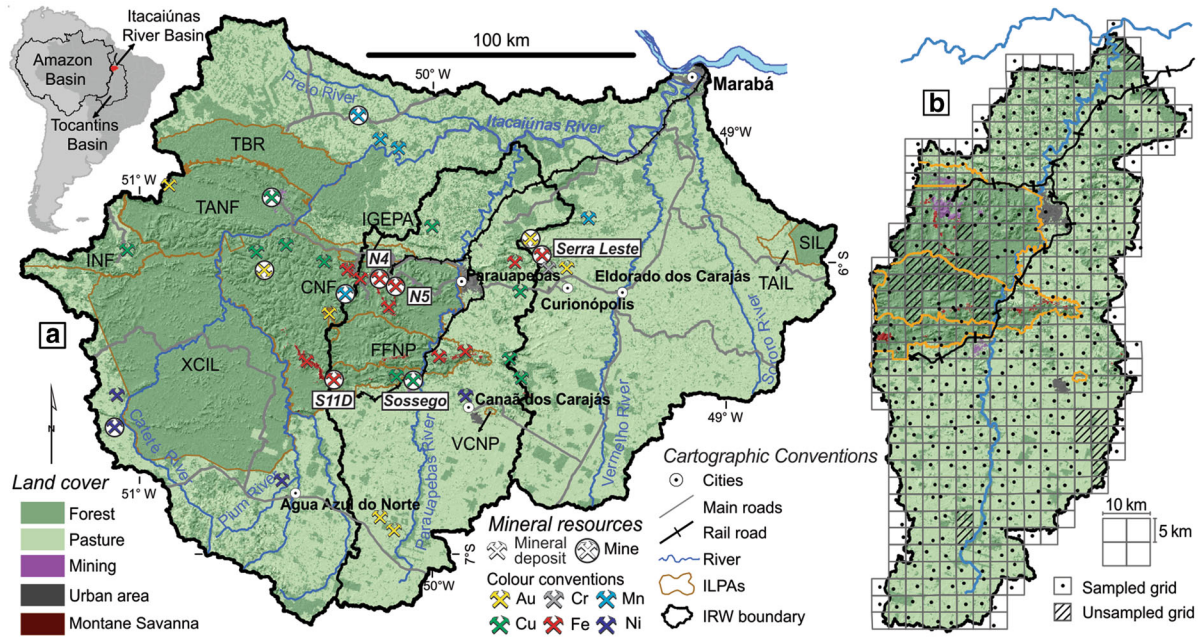

Fig. 1 Map of the Parauapebas sub-basin of the Itacaiúnas River Basin located in the Brazilian Amazonia, Pará state, northern Brazil. The location of main cities and the major land use and land cover, including mines, and mineral deposits, and the indigenous lands and protected areas are indicated in the study area (modified from Souza-Filho et al. 2016); TANF, Taparapé-Aquiri National Forest; XCIL, Xikrin-Cateté Indigenous Land; SIL, Sororó Indigenous Land; TAIL, Tuwa Apekuakawere Indigenous Land; VCNP, Veredas dos Carajás Natural Park; CNF, Carajas National Forest; INF, Itacaiúnas National Forest; TBR, Tapirapé Biological Reserve; and EPAIG, EPA of the Igarapé Gelado

well as help the State's environmental agencies to develop specific regulation reference values for the Amazon.

Study area

The Parauapebas sub-basin (PSB; latitude − 7.168 to − 5.623′S and longitude: − 50.355 to − 49.725′E) in the Itacaiúnas River Basin (IRB) is situated in the State of Pará, in northern Brazil (Fig. 1). This sub-basin covers an area of approximately 9653 km^2, includes the eastern area, and extends to the south and northeast of Serra dos Carajás, a plateau where are located the Carajás National Forest and National Park of Ferruginous Fields (Souza-filho et al. 2016; Pontes et al. 2019). The altitude ranges from 350 to 900 m. The IRB is an economically important region because of several active mines and large cattle production. The sub-basin of IRB selected for the present study is located in the vicinity of the Sossego Copper Mine and comprises parts of the municipalities of Parauapebas, Curionópolis, and Canaã dos Carajás, all drained by the Parauapebas River (Fig. 1). The Parauapebas River is a tributary of the Itacaiúnas River, its headwaters are situated to the east of Serra da Seringa, and it moves in the S–N direction, cutting the Serra dos Carajás and passing immediately to the west of Parauapebas city (Fig. 1).

The region was originally covered by Amazon rainforest and subordinate montane savanna, but land use change has turned it into pasturelands with fragments of remainder tropical rainforest, and minor urban and mining areas (Souza-Filho et al. 2016; Pontes et al. 2019). The area has a humid tropical climate, with an average annual temperature of 27.2 °C and a relative humidity of 90% (Alvares et al. 2013). The rainfall in the region presents a strong seasonal variation between a rainy season (from November to April with average precipitation of ∼ 1550 mm) and a dry season (from May to October with precipitation average of ∼ 350 mm) (de Moraes et al. 2005).

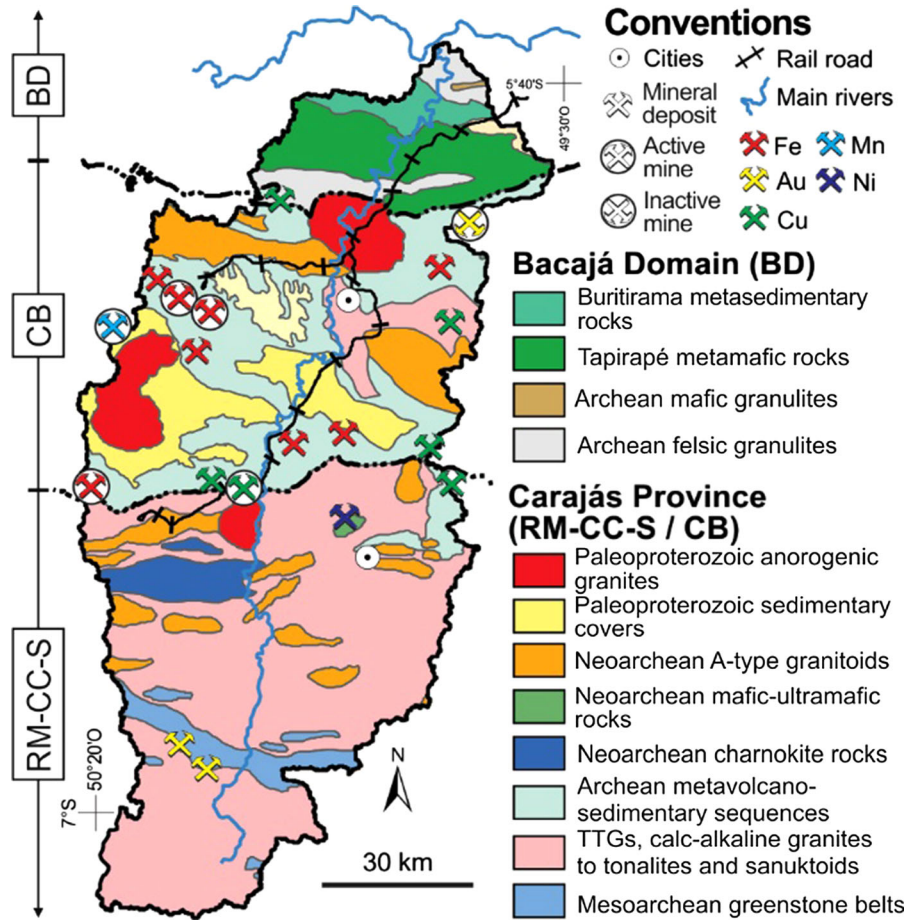

Fig. 2 Simplified geological map of the Parauapebas sub-basin of the Itacaiúnas river basin located in the Carajás region, Pará state, north of Brazil (modified from Vasquez et al. 2008; Dall'Agnol et al. 2017); RM-CC-S (Rio Maria, Sapucaia and Canaã dos Carajás domains) and CB (Carajás Basin)

Geological setting

The geological map of the PSB is shown in Fig. 2 (modified from Vasquez et al. 2008; Dall'Agnol et al. 2017). The Parauapebas River crosses the limit between the Carajás Province and the Bacajá domain of the Transamazonas Province. The northern part of PSB corresponds to the Bacaja domain which consists of Neoarchean to Paleoproterozoic units composed of high-grade metamorphic rocks and metavolcanic and meta-sedimentary rocks. Most of the PSB is situated in the Carajás Province, and the southern part of it is occupied by the Rio Maria, Sapucaia, and Canaã dos Carajás Archean domains that are dominantly composed of Mesoarchean granitoid rocks of diversified composition and subordinate metamafic–ultramafic greenstone belts (Dall'Agnol et al. 2017; Feio et al. 2013; Monteiro et al. 2008). These units are crosscut by Neoarchean granites, mafic charnockites and mafic–ultramafic stratified complex (Vasquez et al. 2008; Feio et al. 2013). In this segment of the basin are located the Sossego copper mine and several other copper deposits (Fig. 1). The center of the PSB corresponds to the Carajás basin, which is mainly constituted of Neoarchean metavolcanosedimentary sequences with dominance of metavolcanic mafic and intermediate rocks and banded-iron formations, which are responsible for the large Fe deposits of Carajás. In the Carajás basin and in the neighbor Mesoarchean terranes are located the Sossego copper mine and several other copper deposits (Fig. 1). Neoarchean granites crosscut the metavolcanosedimentary units, and the Archean units are partially covered by Paleoproterozoic sedimentary units. Paleoproterozoic granite stocks and batholiths are widespread in the Carajás Province (Dall'Agnol et al. 2005; Teixeira et al. 2017) and are intrusive in the Archaean units (Fig. 2). They are anorogenic, A-type granites and, in

geochemical terms, have some analogies with the A-type Neoarchean granitoids (cf. Dall'Agnol et al. 2017).

Materials and methods

Strategies followed for high-density sampling

A total of 727 soil samples were collected at one sample from each 5 × 5 km grid (Fig. 1a, b) as part of a high-density (in a regional-scale) soil sampling survey conducted by Institute Technologic Vale (ITV) in 2017–2018 under the Itacaiúnas Geochemical Mapping and Background Project, ItacGMBP. The locations of the sampling points were determined from a geographic information system, combining data of topography, geology, soil classes, and land use and land cover (Fig. 1). Samples were collected from two depths at each site: surface soil (SS; 364 samples) from 0 to 20 cm and deep soil (DS; 363 samples) from 30 to 50 cm. These depths were chosen to represent soils that have received inputs due to anthropogenic contributions (SS) and those that have not (DS). For each sample, five subsamples were taken within a 5 m × 5 m square and homogenized into a composite sample (approximately 5 kg). Sampling was avoided in areas near potential sources of contamination (near roads, railroads, mining, and urban areas); stainless steel equipment was used for sample collection and preparation.

A computer-based framework was developed in the ItacBGMBP to give support to field and laboratory work for sample collection, data storage, screening, and validation. The framework is composed of three main components: (1) an iPad application for sample collection developed in Swift; (2) a server back-end written in Java which receives data from the iPads in the field and acts as a central repository for sample data sharing and synchronization between different field teams; and (3) data validation and reporting scripts developed in R (R Core Team 2018). Data screening and validation are active within all three components. As an example, the iPad application and the server back-end ensure that only one sample is collected in each quadrangle and in planned locations. Additionally, each sample receives an automatically generated unique code based on its location and type. As laboratory results refer to those sample codes, it is possible to detect eventual laboratory errors, such as results associated with nonexistent sample codes or multiple results associated with the same code.

Laboratory techniques and analytical methods

All soils samples were oven-dried at 70 °C temperature, disaggregated, and passed through an 80 mesh (< 0.177 mm) nylon sieve in order to remove coarser materials. Approx. 50 g of soil was ground and sieved through a 200 mesh (< 75 μm) sieve and stored in polythene bags. Microwave-assisted, aqua regia digestion (EPA, 3051A; 1:3 HCl:HNO3, v/v; USEPA, 2007) of the < 75 μm fraction produced for determination of 51 elements (Al, Ag, As, Au, B, Ba, Be, Bi, Cd, Ce, Ca, Co, Cr, Cs, Cu, Fe, Ga, Ge, Hf, Hg, In, K, La, Li, Mn, Mg, Mo, Na, Nb, Ni, P, Pb, Rb, Re, S, Sb, Sc, Se, Sn, Sr, Ta, Ti, Te, Th, Tl, U, V, W, Y, Zn, Zr) using Inductively Coupled Plasma Mass Spectrometer (ICP-MS) and Inductively Coupled Plasma Atomic Emission Spectrometer (ICP-AES) at the certified laboratory of ALS Brasil Ltda. These results are considered 'pseudototal' because this method is less aggressive than those using other acids which dissolve the entire silicate fraction (Boim et al. 2018). This method is recommended by the Brazilian Council for the Environment to assess potentially toxic concentrations of elements in soil (CONAMA 2009). Quality control was monitored using duplicate samples and replicated analyses of certified standard reference materials (CRMs: GBM303-4, MRGeo08, GBM908-10, SRM88B). The results show good agreement between the CRMs and data obtained in the present work. Precision was checked by calculating the relative standard deviation (% RSD) as determined from the mean and standard deviation of the repeated analysis of reference standards and samples. The RSD was within ± 10% for most of the elements. Five elements presented a large percentages of samples with values below detection limits (DL): Au (> 95%), Re (> 95%), Ta (> 90%), Sb (> 80%), and W (70%); these elements were not used in the further statistical analyses as they provide only limited information.

Statistical methods and background calculation

Statistical treatment was carried out by applying univariate statistics [e.g., descriptive statistics and exploratory data analysis (EDA: histogram, box plots, density plot, and Q–Q plot) and multivariate statistics

(e.g., Spearman correlation, principal component analysis, PCA, and linear discriminant analysis, LDA)] following the standard methods (Reimann et al. 2002; Reimann and de Caritat 2017; Grunsky 2010). The elements with significant numbers of analyses below the detection limit (DL) were discarded and in those with only sporadic values below detection limit were replaced by the respective 1/2 DL. For multivariate analysis, the raw data were transformed using centered log ratio (clr) in order to eliminate closure effect, which 'opens' or 'unconstrains' the data (Aitchison 1986; Filzmoser et al. 2009). The data distribution and assumption of normality for elements were checked on both untransformed and clr-transformed data by using a combination of graphical (e.g., EDA plot) and numerical techniques [e.g., Shapiro–Wilk (S–W) test and Kolmogorov–Smirnov (K–S) test]. The Mann–Whitney *U* test was applied to determine the significant differences for mean values of elements between surface and deep soils. Spearman's correlation was used to identify the relationship between the variables on both the untransformed and clr-transformed data to evaluate closure issues because it is nonparametric and less sensitive to outliers. Subsequently, PCA was used on both log-transformed and clr-transformed data to test the effectiveness of clr transformation over log transformation to provide meaningful insight into geochemical associations.

The geochemical background concentrations were estimated using various recently developed statistical techniques such as 'M_{MAD}', the median + 2 median absolute deviation (MAD); Tukey's inner fence (TIF); the upper whisker of a Tukey's box plot as calculated by the third quartile + 1.5 IQR (interquartile range); and percentile-based approach with 75th, 90th, 95th, and 98th percentile of a given log-transformed dataset. The detailed description of these techniques can be found in Ander et al. (2013), Reimann and Caritat (2017b), and Reimann et al. (2018). All the statistical analysis and background calculations were accomplished with SPSS software (version 18.0) and the free statistical software R version 3.5 (R Core Team 2018).

Geochemical mapping

World Geodetic System 1984 (WGS84) data were used for geochemical and other maps presented here. Spatial distribution pattern of elements in soils is shown using the inverse distance weighted (IDW) interpolation method, and the concentrations of the elements were exhibited according to a graduated color palette based on percentile values of 5, 50, 75, 95, and > 98. All maps were visualized using ArcGIS 10.6 software.

Calculation of contamination indices

The contamination levels in soils were determined using the contamination factor (CF) and degree of contamination (C_{deg}) following the equations proposed by Hakanson (1980). The contamination factor (CF) is a single-metal index, calculated using the following equation (Eq. 1):

$$\mathrm{CF} = \frac{C_{\mathrm{metal}}}{C_{\mathrm{background}}} \tag{1}$$

where C_{metal} is the concentration of an element in the sample and $C_{\mathrm{background}}$ is the background value. For this purpose, conservative BTVs and high BTVs estimated from this study were used. Classification of 'CF' was done according to Hakanson (1980): $\mathrm{CF} < 1$ indicates low contamination, $1 \leq \mathrm{CF} < 3$ is moderate, $3 \leq \mathrm{CF} < 6$ is considerable, and $\mathrm{CF} \geq 6$ is very highly contaminated.

The degree of contamination (C_{deg}) measures the degree of overall contamination for a particular sampling site based on integrating the sum of all CFs. This is calculated using the following formula (Eq. 2) (Hakanson 1980):

$$C_{\mathrm{deg}} = \sum_{i=1}^{n} \mathrm{CF} \tag{2}$$

where n is the number of analyzed pollutants and CF is the contamination factor for each element. The classification of 'C_{deg}' is given by Hakanson (1980) as: $C_{\mathrm{deg}} < 8$, low; $8 \leq C_{\mathrm{deg}} < 16$, moderate; $16 \leq C_{\mathrm{deg}} < 32$, considerable; and $C_{\mathrm{deg}} > 32$, high contamination.

Results

Metal concentrations and distribution in soils

Elemental concentrations, descriptive statistics, Brazilian legislated guidelines ('PV,' prevention, and 'IV,' intervention; CONAMA 2009) and World background levels (Kabata-Pendias and Pendias 1992; Berrow and Reaves 1984) are given in Table 1 (all data shown in Table 1S). For the raw geochemical

Table 1 Statistical summary of chemical compositions (unit: mg/kg) in soils of Parauapebas region from both surface soils (SS; no. of samples 364) and deep soils (DS; no. of samples 363). Detection limit (DL) of major and minor elements (Al, Fe, Ca, Na, Mg, K, S and P) in % while others are in mg/kg

Element	Horizon	DL	% < DL	Min	Avg	Avg*	M	SD	SD*	Max	CV %	K–S Sig.	K–S Sig.*	M–W Sig.	PV	IV	WS
Al	SS	0.01	0	4400	24,810	18,621	17,950	25,072	2.00	202,000	101	0.00	0.00		–	–	–
Al	DS	0.01	0	3100	27,256	20,417	20,500	26,816	2.00	204,000	98	0.00	0.04	S	–	–	–
Fe	SS	0.01	0	3000	49,595	28,840	27,050	58,189	2.88	296,000	117	0.00	0.0		–	–	–
Fe	DS	0.01	0	3000	54,523	32,359	33,200	59,792	2.82	302,000	110	0.00	0.03	NS	–	–	–
Na	SS	0.01	58	<50	72.39	67.61	50	31.1	1.45	300	43	0.00	0.006		–	–	–
Na	DS	0.01	61	<50	71.63	66.07	50	37.1	1.45	500	52	0.00	0.004	NS	–	–	–
Ca	SS	0.01	3.8	<50	882.42	562.34	700	892.9	2.88	10,100	101	0.00	0.00		–	–	–
Ca	DS	0.01	9.6	<50	614.46	389.05	500	569.2	2.88	4300	93	0.00	0.00	S	–	–	–
Mg	SS	0.01	1.6	<50	402.47	218.78	200	996.4	2.45	13,800	248	0.00	0.00		–	–	–
Mg	DS	0.01	3.8	<50	414.05	204.17	200	1117.9	2.57	15,900	270	0.00	0.02	NS	–	–	–
S	SS	0.01	13	<50	194.92	154.88	200	145.5	2.00	1100	75	0.00	0.02		–	–	–
S	DS	0.01	30	<50	156.20	114.82	100	152.9	2.09	1200	98	0.00	**0.05**	S	–	–	–
P	SS	10	0	20	243.32	199.53	200	174.4	1.86	1490	72	0.00	**0.56**		–	–	–
P	DS	10	0	20	204.08	154.88	160	168.4	2.04	1310	83	0.00	**0.06**	S	–	–	–
Mn	SS	5	0	13	606.20	316.23	308	941.5	3.09	8590	155	0.00	**0.51**		–	–	571
Mn	DS	5	0	23	527.38	257.04	245	903.4	3.16	8200	171	0.00	**0.42**	S	–	–	
As	SS	0.1	5.2	<0.05	1.24	0.52	0.5	2.9	3.47	38.4	231	0.00	0.003		–	–	11.4
As	DS	0.1	4.1	<0.05	1.35	0.62	0.5	2.9	3.24	37.1	215	0.00	0.04	NS	–	–	–
Ba	SS	10	10	<5	65.87	38.02	50	67.2	3.16	420	102	0.00	0.00		150	300	–
Ba	DS	10	11	<5	57.55	33.11	40	62.0	3.09	390	108	0.00	0.04	NS	–	–	–
Be	SS	0.05	7	<0.02	0.28	0.18	0.17	0.3	2.63	2.43	111	0.00	**0.17**		–	–	–
Be	DS	0.05	7	<0.02	0.30	0.19	0.19	0.3	2.69	2.54	110	0.00	**0.21**	NS	–	–	–
Bi	SS	0.01	0.5	<0.01	0.12	0.06	0.06	0.2	2.95	1.3	125	0.00	0.05		–	–	–
Bi	DS	0.01	0	<0.01	0.13	0.07	0.06	0.2	2.95	1.34	123	0.00	**0.09**	NS	–	–	–
Cd	SS	0.01	15	<0.01	0.03	0.02	0.02	0.1	2.45	0.44	167	0.00	**0.16**		1.3	3	0.49
Cd	DS	0.01	26	<0.01	0.02	0.01	0.01	0.0	2.34	0.35	200	0.00	0.00	S	–	–	–
Ce	SS	0.02	1.5	<0.01	45.65	20.89	24.35	62.9	4.68	490	138	0.00	0.00		–	–	–
Ce	DS	0.02	1.5	<0.01	51.80	23.44	27.8	71.6	4.90	490	138	0.00	0.03	NS	–	–	–
Co	SS	0.01	0	0.2	10.71	3.47	2.9	22.6	4.27	237	211	0.00	**0.09**		25	35	
Co	DS	0.01	0	0.2	10.65	3.39	2.7	22.7	4.37	239	213	0.00	0.02	NS			
Cr	SS	1	0	2	82.34	26.92	31	296.3	3.89	3970	360	0.00	**0.07**		75	150	70.9
Cr	DS	1	0	1	90.84	30.20	36	309.5	3.98	3950	341	0.00	0.05	NS			

Table 1 continued

Element	Horizon	DL	% < DL	Min	Avg	Avg*	M	SD	SD*	Max	CV %	K–S Sig.	K–S Sig.*	M–W Sig.	PV	IV	WS
Cs	SS	0.05	0.5	0.02	0.49	0.34	0.33	0.7	2.24	11.25	145	0.00	**0.2**				
Cs	DS	0.05	1	<0.02	0.50	0.35	0.34	0.7	2.29	11.45	146	0.00	**0.14**	NS			
Cu	SS	0.2	0	0.5	48.88	21.38	21.8	79.0	3.80	726	162	0.00	**0.92**		60	200	28.2
Cu	DS	0.2	0	0.3	53.27	21.88	24.6	88.2	4.17	941	166	0.00	**0.88**	NS	–	–	–
Ga	SS	0.05	0	1.64	11.88	8.91	8.7	10.1	2.19	68.3	85	0.00	**0.35**		–	–	–
Ga	DS	0.05	0	0.92	13.15	9.77	10.15	10.7	2.19	69.7	81	0.00	**0.44**	S	–	–	–
Hf	SS	0.02	1.5	<0.01	0.16	0.08	0.07	0.3	2.82	2.17	188	0.00	0.00		–	–	–
Hf	DS	0.02	1	<0.01	0.19	0.10	0.08	0.3	2.82	2.27	168	0.00	0.00	S	–	–	–
Hg	SS	0.01	0	0.02	0.10	0.08	0.07	0.1	1.95	0.54	70	0.00	**0.2**				0.06
Hg	DS	0.01	0	0.01	0.10	0.07	0.07	0.1	2.09	0.6	80	0.00	**0.3**	NS	–	–	–
K	SS	0.01	0.5	<50	493.41	316.23	300	662.7	2.45	8300	134	0.00	**0.2**		–	–	–
K	DS	0.01	0.2	<50	484.44	288.40	200	698.0	2.57	8700	144	0.00	**0.4**	NS	–	–	–
La	SS	0.2	0	0.5	16.09	7.24	7.2	25.3	3.55	250	157	0.00	0.015		–	–	–
La	DS	0.2	0	0.5	16.46	7.41	7.2	27.0	3.47	250	164	0.00	0.015	NS	–	–	–
Mo	SS	0.05	0.5	<0.02	0.85	0.52	0.48	0.9	2.75	6.34	108	0.00	**0.2**		30	50	
Mo	DS	0.05	0.2	<0.02	0.92	0.55	0.53	1.0	2.82	6.59	109	0.00	**0.15**	NS	–	–	–
Nb	SS	0.05	0.5	<0.02	1.03	0.52	0.5	1.5	3.09	10.7	150	0.00	0.00		–	–	–
Nb	DS	0.05	1	<0.02	0.96	0.51	0.46	1.4	2.95	8.29	142	0.00	0.00	NS	–	–	–
Ni	SS	0.2	0	0.7	21.47	7.24	6.3	87.8	3.24	1260	409	0.00	0.015		30	70	17.8
Ni	DS	0.2	0	0.7	21.95	7.41	6.6	87.6	3.31	1230	399	0.00	0.01	NS			
Pb	SS	0.2	0	1.1	8.78	6.61	6.35	7.6	2.09	43.8	86	0.00	**0.34**		72	180	28.4
Pb	DS	0.2	0	1.3	9.01	6.92	6.6	7.6	2.04	44.6	85	0.00	**0.22**	NS	–	–	–
Rb	SS	0.1	0	0.2	11.42	6.03	6.5	17.1	3.24	152	149	0.00	0.00		–	–	–
Rb	DS	0.1	0	0.2	11.33	5.62	6	17.4	3.47	162	154	0.00	**0.26**	NS	–	–	–
Sc	SS	0.1	0	0.3	8.29	4.57	4.85	8.8	3.31	53.1	106	0.00	0.006		–	–	–
Sc	DS	0.1	0	0.3	9.49	5.37	6.1	9.5	3.31	54.1	100	0.00	0.002	NS	–	–	–
Sr	SS	0.2	0	0.7	9.46	6.31	6.7	9.2	2.57	58.4	97	0.00	**0.22**		–	–	–
Sr	DS	0.2	0	0.6	7.28	4.79	5	7.3	2.57	48.5	101	0.00	**0.24**	S	–	–	–
Th	SS	0.2	0	0.3	14.11	7.08	6.55	21.8	3.16	202	155	0.00	0.16		–	–	–
Th	DS	0.2	0	0.4	16.41	8.51	7.8	24.7	3.09	222	151	0.00	0.02	S	–	–	–
Ti	SS	0.005	8	<25	423.09	239.88	250	481.2	3.16	2920	114	0.00	0.034		–	–	–
Ti	DS	0.005	6.5	<25	468.97	269.15	290	503.8	3.09	3080	107	0.00	0.04	NS	–	–	–
U	SS	0.05	0	0.06	1.93	1.00	0.95	3.3	2.95	28.4	170	0.00	0.00		–	–	–

Table 1 continued

Element	Horizon	DL	% < DL	Min	Avg	Avg*	M	SD	SD*	Max	CV %	K–S Sig.	K–S Sig.*	M–W Sig.	PV	IV	WS
U	DS	0.05	0	0.06	2.20	1.12	1.07	3.7	2.95	31.6	169	0.00	0.00	NS	–	–	–
V	SS	1	0	<1	81.09	42.66	43	87.3	3.39	435	108	0.00	0.03		–	–	–
V	DS	1	0	2	90.21	48.98	52	91.3	3.39	431	101	0.00	0.02	NS	–	–	–
Y	SS	0.05	0	0.14	7.01	2.51	2.2	11.6	4.27	85.5	166	0.00	0.03		–	–	–
Y	DS	0.05	0	0.13	7.11	2.63	2.27	11.8	4.17	85.9	166	0.00	0.06	NS	–	–	–
Zn	SS	2	0.5	<1	22.35	15.85	16	25.7	2.19	202	115	0.00	0.2		300	450	67.8
Zn	DS	2	0.5	1	20.85	14.79	15	24.9	2.19	217	119	0.00	0.32	NS	–	–	–
Zr	SS	0.5	1	<0.25	6.48	2.69	2.1	13.1	3.24	91.1	202	0.00	0.00		–	–	–
Zr	DS	0.5	0.8	<0.25	7.73	3.55	3	14.1	3.09	95.4	183	0.00	0.02	S	–	–	–
B	SS	10	63	<5	6.88	6.46	5	2.8	1.41	30	40	0.00	0.32		–	–	–
B	DS	10	66	<5	6.75	6.31	5	2.9	1.41	30	43	0.00	0.55	NS	–	–	–
Se	SS	0.2	10	<0.1	0.66	0.34	0.1	0.7	3.47	4	102	0.00	0.00		–	–	–
Se	DS	0.2	9.8	<0.1	0.63	0.33	0.1	0.6	3.39	4	102	0.00	0.00	NS	–	–	–
Sn	SS	0.2	2	<0.1	1.31	0.78	0.7	1.6	2.69	16	125	0.00	0.00		–	–	–
Sn	DS	0.2	1	<0.1	1.42	0.87	0.8	1.7	2.63	15.9	121	0.00	0.00	NS	–	–	–

SS, surface soils; DS, deep soils; DL, detection limit; Min, minimum; Max, maximum; Avg, average; M, median; SD, standard deviation; CV, coefficient of variation; K–S Sig, Kolmogorov–Smirnov normality test on raw data; and K–S Sig*, Kolmogorov–Smirnov normality test on clr-transformed data; Avg* and SD* are calculated based on log transformed data; -, data not available

Bold: normal distribution at $p > 0.05$. M–W Sig.: The Mann–Whitney U test; S: values < 0.05 for the asymp.sig. (two-tailed) are significantly different; NS: values > 0.05 for the asymp.sig. (two-tailed) are not significantly different; PV and IV are prevention and intervention values established in Brazilian legislation (CONAMA 2009); and WS is background value of world soils (Kabata-Pendias and Pendias 1992; Berrow and Reaves 1984)

data, the mean and median values of most of the elements show significant variation and have also higher standard deviations, indicating that these elements are asymmetrically distributed. The Kolmogorov–Smirnov (K–S) test results (Table 1) also show that most of the original compositions are not normally distributed, as the asymptotic significance (α) values were equal to 0.00, which is less than the critical level of significance $\alpha = 0.05$. These distributions were significantly improved after clr transformation (Table 1; some selective examples are shown in EDA plot, Fig. 1SM), but not all elemental distributions conformed to normality even after clr transformation, confirming the fact that a normal distribution is not typical of geochemical data. This may be due to the presence of multiple populations and outliers as a result of mixed origins and influences of various lithological or geochemical processes on the data (Zuo et al. 2009). The coefficient of variation (CV) varied from 40 to 409%, indicating a high degree of variability (CV > 100%) for most of the elements, except Na, B, Ga, Hg, P, Pb, and S.

The Mann–Whitney *U* test was used to compare the similarity between the surface and deep soils (Table 1). The results show that, for most of the elements, the asymptotic significance, α, was > 0.05, which indicates they are not significantly different (NS) at 95% confidence interval. Moreover, the quartile distribution of elements between surface and deep soils was nearly similar, although the median values vary slightly for some elements, e.g., Zr, U, Th, Sr, Cd, Cr, Ga, Ba, P (Fig. 3). When compared with the CONAMA regulations, the average concentrations for most all elements were below the PV and IV limits, except Cr, which exceeded the PV limit (Table 1). However, when the maximum concentrations are considered, Ba, Co, Cr, Cu, and Ni exceeded both limits. When compared with the background soils, it can be observed that average concentrations of As, Cd, and Zn are below the world averages, while Cr, Cu, Ni, and Mn exceeded world averages.

Figure 4 shows the spatial distribution of selected elements (Fe, Mn, Ba, Pb, Cu, Ni, Cr, and V) in surface and deep soils; their patterns are very similar between

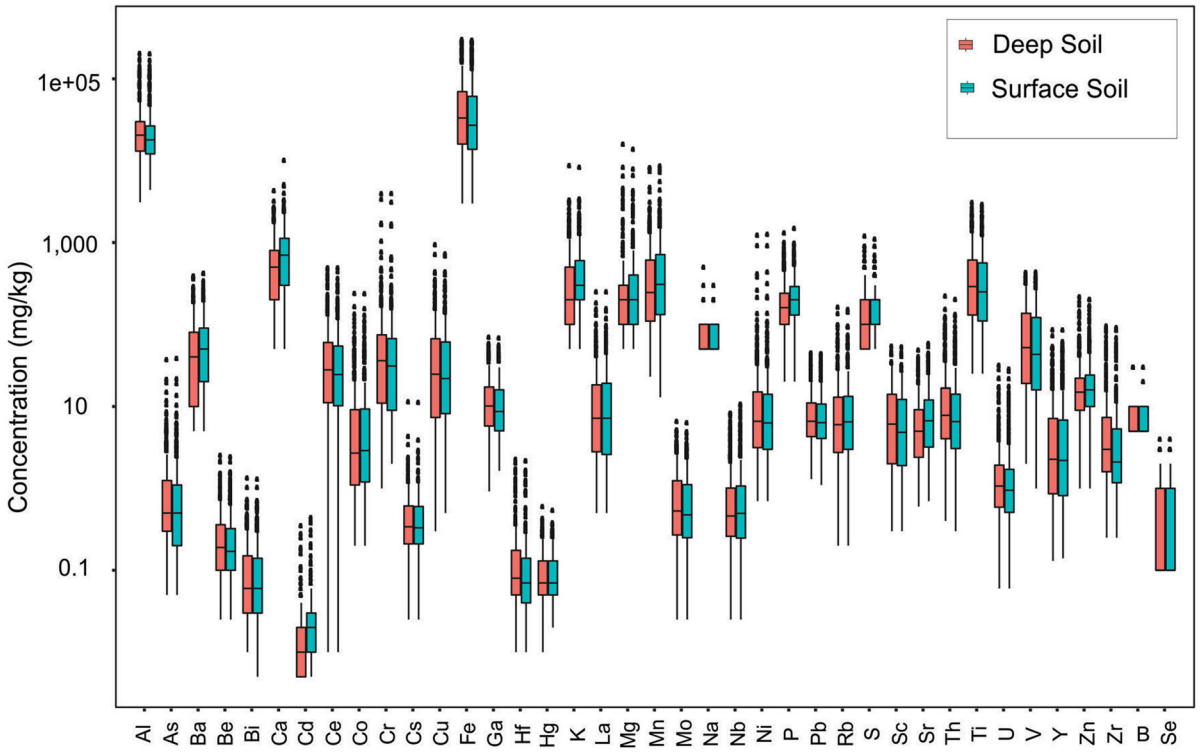

Fig. 3 Boxplots for elements showing the distribution of chemical elements in surface and deep soils. The box indicates approximately the 25th, 50th (median = black line) and 75th percentile; outliers (marked with points) are defined according to: (upper whisker, lower whisker) = (upper hinge, lower hinge) ± 1.5 × hinge width

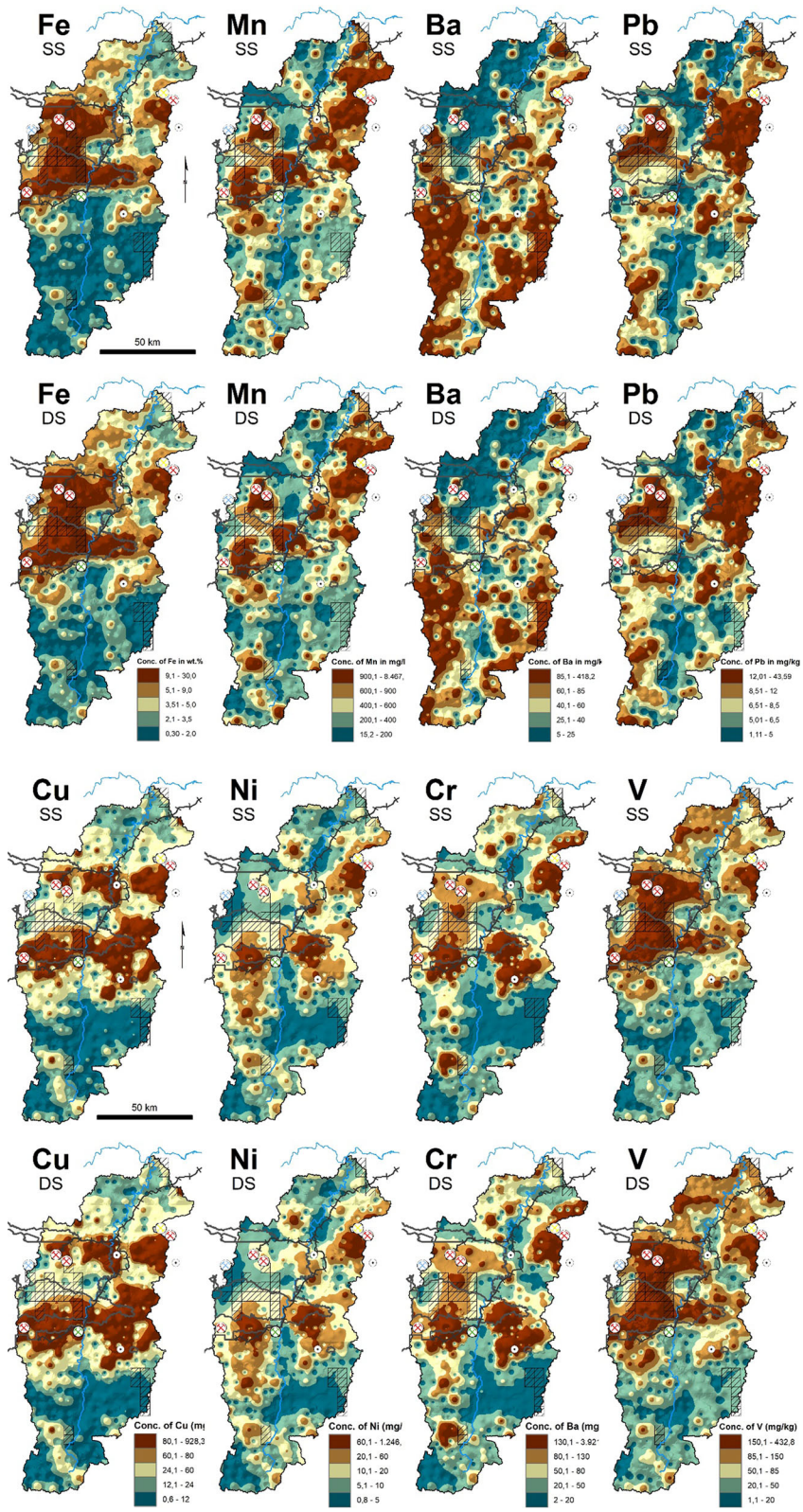

Fig. 4 Spatial distribution of Fe, Mn, Ba, Pb, Cu, Ni, Cr, and V in surface soil (SS) and deep soils (DS) of the Parauapebas basin. Refer to Fig. 2 for concentrations with respect to geological domains

the two horizons, but varied with respect to geological domains. Iron was mainly enriched in the Carajás basin while lower concentrations were obtained in the Rio Maria, Sapucaia, and Canaã dos Carajás domains. Manganese is not associated with Fe in these soils (as might be expected) (Fig. 4). The patterns of Cr and Ni are strongly correlated, and their higher contents are mainly registered in the Carajás basin and in the Sapucaia greenstone belt. Copper shows also higher concentration in the Carajás basin but it differs from Ni and Cr because it follows preferentially the north and south copper belts. The distribution pattern of V approaches in some areas those of Ni and Cr, but it is more closely related to Fe (Fig. 4). Barium differs of all these elements because it shows higher contents in soils of the Canaã dos Carajás, Sapucaia, and Rio Maria domains, which indicates that it is probably linked with Archean granitoids that are dominant there (Fig. 2). Although Pb is enriched in the Carajás basin, its distribution pattern is distinct from other elements.

Correlation and PCA analysis

Spearman's correlation coefficients ($p < 0.05$) were calculated for all elements on log-transformed data (Fig. 5). Correlations were classified as: strong ($r = \pm 0.7$ to ± 0.9); moderate ($r = \pm 0.4$ to ± 0.69); weak ($r = \pm 0.1$ to ± 0.39); and none or very weak (0 to ± 0.1) (Schober et al. 2018). Strong positive correlations include the group Cr, Ni, V, P, Cu, Fe, Sc, and Ti; the group Al, Ga, LOI, Zr, Hf, As, Hg, and Mo; Al with V, Fe, and Sc; the group Ca, Mg, K, Rb, and Ba; and the group Mn, Co and Zn; additional strong correlation was observed between Y–La, Zr–Hf, Sr–Ba, Co–Ni, Al–LOI. Fe and Mn are poorly correlated.

PCA results (Fig. 6a, b) between log- and clr-transformed data are significantly different, with clr-transformed data resulting in better separation between variables. In clr-transformed PCA, five principal components (PCs) with eigenvalues > 1 were extracted, describing 71.68% of the total variance. The first two PCA axes together accounted for 46.6% (Dim 1—32.5% and Dim 2—14.1%) of the total variance. The elements assembled around each PC with significant loadings formed four major elemental groups (Fig. 6). The first group (Gp-1) is comprised of Ti, Fe, V, Sc, Cu, Cr, and Ni which were mostly + vely associated with Dim 1 and − vely with Dim 2. In the second group (Gp-2), Al, Ga, Zr, Hf, Th, Nb, U, Th, and P, which were + vely loaded with both Dim 1 and Dim 2, are associated. Elements such as Rb, Sr, B, Na, Ca, Mg, K, Cs, and Ba are assembled in Gp-3 and were + vely loaded with Dim 2, but − vely loaded with Dim 1. In addition, Gp-4 is constituted of Mn, Co, Y, La, Ce, Zn, Be, and Cd that has negative loading with both Dim 1 and Dim 2.

PCA (Fig. 7a) was also applied to delineate the geochemical relationship between surface and deep soils, which are geochemically similar. This was further evaluated using linear discriminant analysis (LDA; Fig. 7b), which demonstrates that the soils of the main geological domains of the studied area can be distinguished based on their geochemical characteristics.

Background threshold values

Table 2 gives the background threshold values (BTVs) of various elements for surface soils (SS) and deep soils (DS), calculated using different methods such as median + 2MAD (M_{MAD}), percentiles (75th, 95th, and 98th), and TIF. The estimation of baseline values by different techniques is strongly dependent of the % of analytical results $<$ DL (Table 2). For example, the estimation of BTV of Se and B by M_{MAD} technique was strongly limited due to the high percentage of results below the detection limit for these elements (Table 1).

The estimated BTVs show small difference between SS and DS for most of the elements (Table 2), making them more suitable for using percentile techniques; however, for M_{MAD} and TIF, some elements such as Ba, Cu, Al, Fe show considerable variations. Furthermore, between methods the BTVs varied significantly (Table 2). The 75th percentile (Q75) produced the lowest values, while TIF gave the highest values, many of them higher than the 98th percentile, and in some cases exceeding the respective maximum values, e.g., Fe, Ba, Cu, Mo, Pb, V, and Se. The M_{MAD}-estimated values lie somewhere between the 95th and 98th percentiles, except Cr, Cu, Mn, Fe, and Mo for which M_{MAD} exceeded the 98th percentile. In a few cases, it also exceeded the respective maximum values, for example, Ba and V. For both SS and DS, the lowest values estimated by the '75th percentile' were considered as conservative BTVs, while 'M_{MAD}' was considered as high BTV, except for

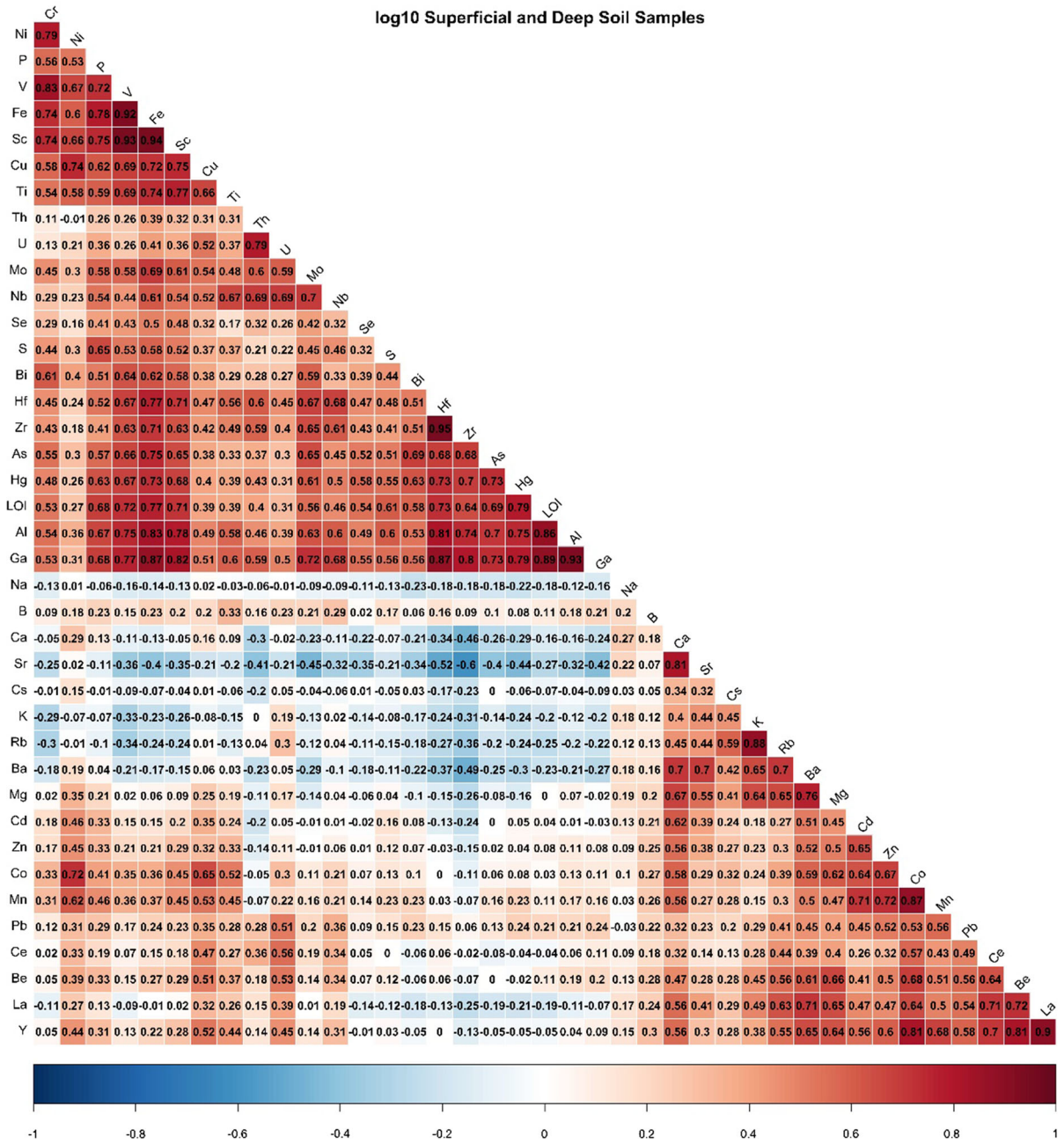

Fig. 5 Spearman's correlation coefficient matrix for elements and LOI based on log-transformed data in soils from Parauapebas basin

Ba and V, which were assumed the Q98 value (see "Discussion" for the reason these methods were used). The conservative and high BTVs were marked in italic and bold, respectively in Table 2. The background values of elements in this study were also compared with those obtained in other Brazilian soils (Table 3).

Environmental pollution level assessment

The CF and C_{deg} values were calculated using the conservative BTV and high BTVs for ten PTEs (Ba, Co, Cr, Cu, Fe, Mn, Ni, Pb, V, and Zn) and are presented in Table 4 and Figs. 8 and 3SM. The CF values varied widely between elements and also varied significantly

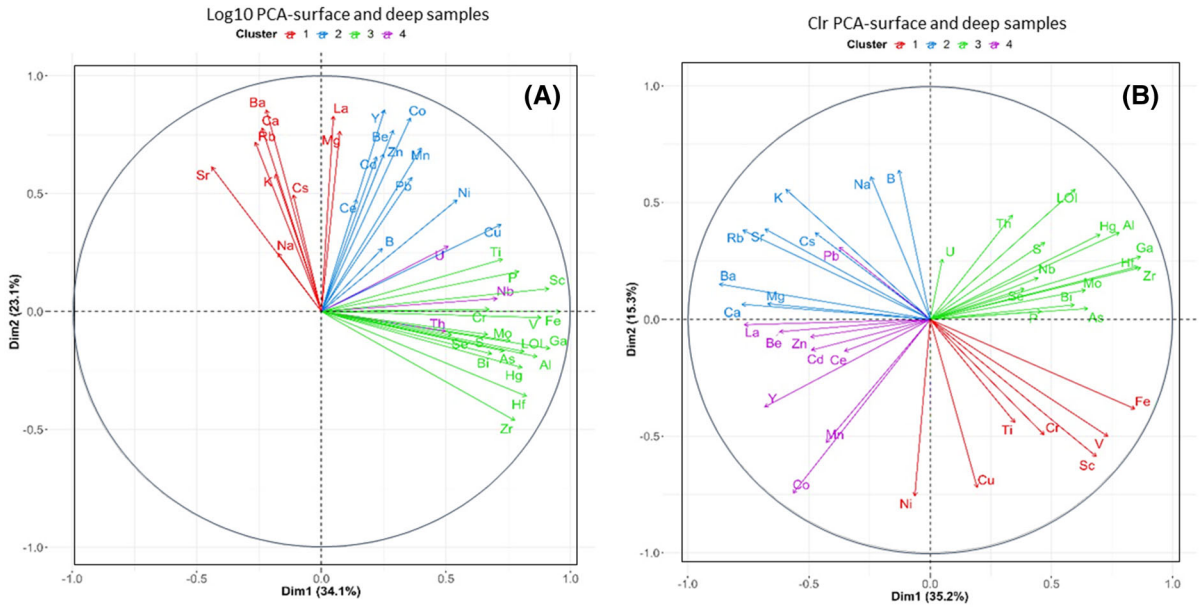

Fig. 6 PCA biplot (Dim 1 vs. Dim 2) showing the differences in geochemical associations between log-transformed (**a**) and centered log-ratio (clr)-transformed (**b**) elemental data for soils from the Parauapebas basin

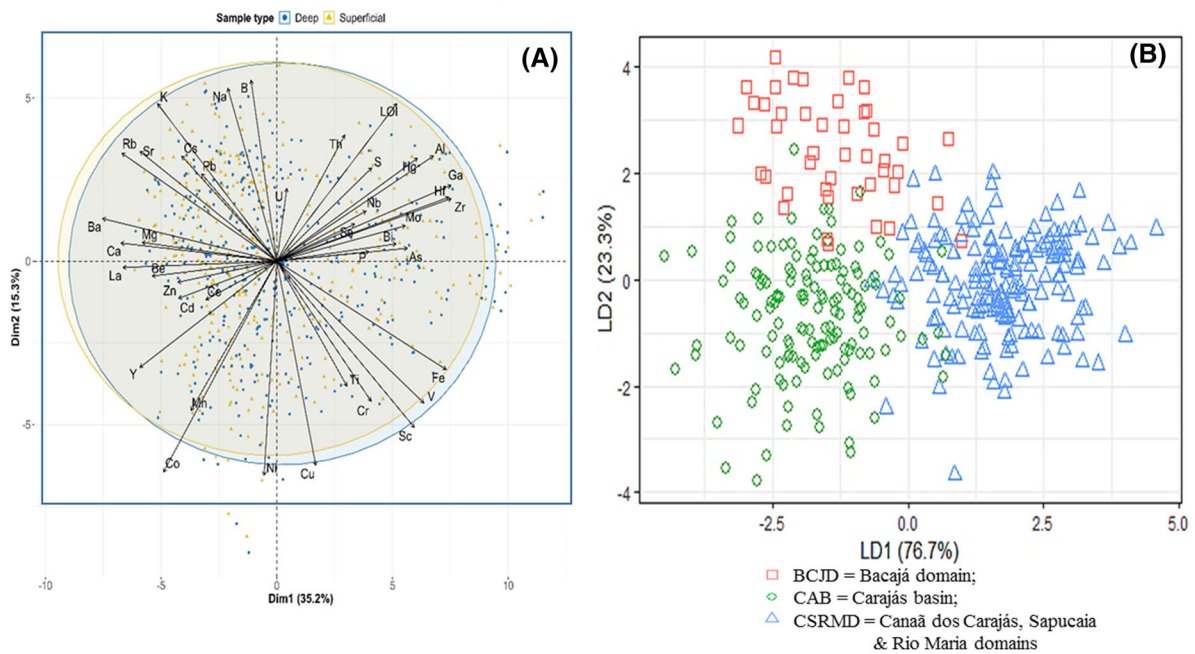

Fig. 7 PCA biplot (Dim 1 vs. Dim 2) **a** showing the geochemical relationships between surface and deep soils; **b** linear discriminate analysis (LDA) showing the geochemical differences of soils from the main geological domains of the studied area

with respect to the type of BTVs used. Higher values were estimated when used conservative BTV, but the values were nearly similar between surface and deep soils. When calculated using the 'conservative' BTVs, in surface soils the maximum CF decreased in the following order: Ni > Cr > Co > Mn > Cu > Fe > Zn > Ba > Pb > V, and for deep soils: Ni > Cr > Co > Cu > Mn > Zn > Fe > Ba > Pb > V. The C_{deg}

Table 2 Geochemical background threshold values (upper limit; mg/kg) of elements in soils of the Parauapebas region obtained from various statistical methods [Median + 2 MAD (M_{MAD}), Tukey's inner fences (TIF) and percentiles (Q75, Q95, Q98)]; Q5 can be referred to lower limit; mg/kg)

Parameter	Types	Nos.	Q5	Q75	Q95	Q98	M_{MAD}	TIF	No. of samples exceeding					
									Q75	Q98	M_{MAD}	TIF	PV	IV
Al	SS	364	6457	*26,303*	83,176	112,202	**56,234**	85,114	92	7	25	17	–	–
Al	DS	363	6761	*30,200*	87,096	120,226	**67,608**	104,713	87	8	24	14	–	–
Fe	SS	364	5754	*61,660*	181,970	245,471	**257,040**	***582,103***	90	8	7	0	–	–
Fe	DS	363	5370	*69,183*	186,209	257,040	**301,995**	***630,957***	92	8	1	0	–	–
As	SS	364	0.05	*1.10*	4.47	7.24	**7.24**	14.13	86	8	8	3	–	–
As	DS	363	0.10	*1.26*	4.90	7.76	**3.98**	10.72	91	8	22	5	–	–
Ba	SS	364	5.01	*89.13*	199.53	**257.04**	***660.69***	***841.40***	104	8	0	0	34	4
Ba	DS	363	5.01	*79.43*	181.97	**229.09**	***316.23***	***1778.28***	94	9	3	0	27	3
Cd	SS	364	0.01	*0.03*	0.08	0.14	**0.16**	0.16	71	8	7	7	0	0
Cd	DS	363	0.01	*0.02*	0.06	0.15	**0.08**	0.16	73	8	11	6	0	0
Co	SS	364	0.40	*9.33*	47.86	79.43	**69.18**	201.84	91	8	10	1	40	31
Co	DS	363	0.40	*9.12*	47.86	69.18	**67.61**	218.78	91	9	9	1	41	31
Cr	SS	364	3.02	*67.61*	190.55	467.74	**562.34**	1412.54	90	8	7	4	83	27
Cr	DS	363	3.02	*74.13*	213.80	478.63	**691.83**	1303.17	91	8	6	4	90	30
Cu	SS	364	2.34	*60.26*	162.18	275.42	**398.11**	***1216.19***	93	8	4	0	93	14
Cu	DS	363	2.29	*66.07*	186.21	302.00	**588.84**	***1757.92***	92	7	2	0	97	16
Mn	SS	364	56.23	*707.95*	1995.26	2884.03	**3890.45**	8810.49	94	8	5	0	–	–
Mn	DS	363	48.98	*602.56*	1778.28	2630.27	**2951.21**	7762.47	95	7	6	2	–	–
Mo	SS	364	0.11	*1.12*	2.88	3.31	**4.79**	***10.59***	90	8	2	0	0	0
Mo	DS	363	0.11	*1.23*	3.09	3.80	**5.01**	***12.02***	91	8	3	0	0	0
Ni	SS	364	1.41	*14.13*	52.48	107.15	**60.26**	142.89	90	8	17	6	39	15
Ni	DS	363	1.32	*15.14*	53.70	109.65	**63.10**	158.49	90	8	15	6	44	13
Pb	SS	364	2.19	*10.72*	25.12	33.88	**27.54**	43.71	91	8	17	0	0	0
Pb	DS	363	2.09	*10.96*	26.92	33.88	**27.54**	44.19	92	8	18	0	0	0
U	SS	364	0.17	*1.70*	6.92	12.59	**5.75**	10.23	91	8	23	13	–	–
U	DS	363	0.20	*1.91*	7.76	14.79	**6.17**	11.09	92	8	26	16	–	–
V	SS	364	6.03	*120.23*	269.15	**331.13**	***891.25***	***2511.89***	92	8	0	0	–	–
V	DS	363	6.03	*138.04*	281.84	**338.84**	***954.99***	***2691.53***	88	8	0	0	–	–
Zn	SS	364	5.01	*23.99*	64.57	114.82	**63.10**	89.13	98	8	19	10	0	0
Zn	DS	363	5.01	*21.88*	58.88	104.71	**50.12**	84.14	93	8	24	11	0	0
B	SS	364	5.01	*10.00*	10.00	10.00	–	28.18	2	2	–	1	–	–
B	DS	363	5.01	*10.00*	10.00	10.00	–	28.18	2	2	–	2	–	–
Se	SS	364	0.10	*1.00*	2.00	2.00	–	***31.62***	38	4	–	0	–	–
Se	DS	363	0.10	*1.00*	2.00	2.00	–	***31.62***	29	4	–	0	–	–
Sn	SS	364	0.20	*1.51*	4.17	5.75	**5.62**	11.22	92	7	25	17	–	–
Sn	DS	363	0.20	*1.70*	4.27	6.31	**6.31**	14.96	87	8	24	14	–	–

Italic: conservative BTV; Bold: high BTV; PV and IV are prevention and intervention limits, respectively, established in Brazilian legislation (CONAMA 2009). Bold italics: overestimated values; - data not available

SS, surface soils; DS, deep soils

Table 3 Comparison between the background values (unit: mg/kg, except Fe in wt.%) of Parauapebas basin and other Brazilian regions (Based on Fernandes et al. 2018, Nascimento et al. 2018, with additional information)

Regions/States of Brazil	Fe	As	Ba	Cd	Co	Cr	Cu	Hg	Mn	Mo	Ni	Pb	Zn
PV[a]	–	15	150	1.3	25	75	60	–	–	30	30	72	300
IV[a]	–	35	300	3	35	150	200	–	–	50	70	180	450
Mato Grosso and Rondônia (MT-RO)[1]	–	–	–	< LD	15.8	39.4	16.5	–	–	–	1.3	8.1	6.8
São Paulo (SP)[2]	.	3.5	75	< 0.5	–	40	35	0.05	–	< 4	13	17	60
Paraíba (PB)[3]	13	0.5	–	0.08	–	15	3.5	0.04	91.8	–	3.3	13	30
Pernambuco (PE)[4]	–	0.6	84	0.68	3.5	35	5	0.01	160	–	8.5	11	34.5
Espírito Santo (ES)[5]	–	12.8	–	< 0.1	10.2	59.1	5.9	–	137	1.7	9.2	< 4.5	29.9
Minas Gerais (MG)[5]		8	93	< 0.4	6	75	49	0.05	–	< 0.9	21.5	19.5	–
Minas Gerais (MG)[5,a]	83		171	1.01	17.5	86.5	13.2		447		23	15.8	31
Pará (PA)[6]	7.1	1.4	14.3	0.4	–	24.1	9.9	0.26	72	0.05	1.4	4.8	7.2
Northern region[7]	10.1	–	–	0.3	1.7	26.8	1.1	–	49	–	6.6		7.7
Southwestern Amazon[8]	15.4	–	16.5	0.1		6.9	2.8	–	13.4	–	1.7	4.4	5.7
Paraiba (PB)[9]	18.7	–	87.96	0.06	7.93	28.8	11.22	–	350	< 0.24	9.12	10.01	23.46
Fernando de Noronha[10]	–	–	834		19.6	266	41.49	–	–	–	58.7		117.5
Rio Grande do Norte (RN)[11]	–	–	58.9	0.1	15.4	30.9	13.7	–	–	–	19.8	16.1	23.85
Parauapebas_SS[12]	6.1	1.1	90	0.03	9.33	67	60.8	0.13	712	1.1	14.1	10.7	24
Parauapebas_DS[12]	6.9	1.25	80	0.02	9.15	74	66.7	0.13	609	1.24	15.1	11.05	22

[a]CONAMA (2009); [1]Santos and Alleoni (2013), 75th percentile; [2]Cetesb (2005), 75th percentile; [3]Silva et al. (2015), 75th percentile; [4]Fernandes et al., 2018 and reference therein, 75th percentile; [5]Paye et al. (2010), 75th percentile; [5]*Caires (2009); [6]Fernandes et al. (2018),75th percentile; [7]Fadigas et al. (2010); mean; [8]Nascimento et al. (2018), 75th percentile; [9]Almeida Júnior et al. (2016), 75th percentile; [10]Fabrício Neta (2012), 75th percentile; [11]Preston et al. (2014); [12]present study, 75th percentile; '–' data not available

values between surface and deep soils were very similar but were different related to the type of BTVs used: varying from 0.93 to 168 (with an average of 9.94) and from 0.92 to 172 (with an average of 9.67), respectively, based on the conservative BTVs and ranging from 0.28 to 32.9 (with an average of 2.38) and 0.28 to 33 (with an average of 2.32), respectively, based on high BTV. The higher values of C_{deg} were found in the Carajás basin, followed by the Bacajá domain. The lower C_{deg} values were obtained in the Canaã dos Carajás/Sapucaia/Rio Maria domains (Fig. 8). The wide variation of C_{deg} values indicates differences in the contamination level of these metals in the space of the PSB.

Discussion

Vertical distribution of elements and evaluation of geogenic versus anthropogenic influence in soil geochemistry

Given that surface soils typically are more impacted by anthropogenic activity and that deep soils are influenced more by geogenic processes (Facchinelli et al. 2001), this distinction can be used to evaluate environmental impact via human activity. It also allows us to identify sites that are contaminated relative to those that are unaffected and to investigate the relationship between the soil depths (Deschenes et al. 2013; Gregorauskienė and Kadūnas 2006). Based on the Mann–Whitney U test (Table 1), it is evident that there is no significant difference between the two horizons for most of the elements. Furthermore, very similar spatial distributions (Fig. 4) between surface and deep soils for most of the elements are an indication of geogenic control, which is consistent with the PCA of clr-transformed data (Figs. 7a, 2SM).

The data clearly indicate that anthropogenic influence has had little or no impact on these soils and that their geochemistry is controlled by geogenic factors, mainly parent materials and weathering processes. However, slight variation in median concentrations (which is a statistically more robust measure of central tendency and more suitable for comparison purposes; Reimann et al. 2005) of some elements between the

Table 4 Contamination factor (CF) and degree of contamination (C_{deg}) calculated for potentially toxic elements in surface and deep soils of the Parauapebas basin

	Ba^a	Ba^b	Co^a	Co^b	Cr^a	Cr^b	Cu^a	Cu^b	Fe^a	Fe^b	Mn^a	Mn^b	Ni^a	Ni^b	Pb^a	Pb^b	V^a	V^b	Zn^a	Zn^b	C^a_{deg}	C^b_{deg}
Surface soils																						
Min	0.1	0.0	0.0	0.0	0.0	0.0	0.0	0.0	0.0	0.0	0.0	0.0	0.0	0.0	0.1	0.0	0.0	0.0	0.0	0.0	0.9	0.3
Max	4.7	1.6	25.5	3.4	59.3	7.1	11.9	1.8	4.9	1.2	12.1	2.2	89.4	20.9	4.1	1.6	3.6	1.3	8.4	3.2	168.1	32.9
Avg	0.7	0.3	1.2	0.2	1.4	0.2	0.8	0.1	0.8	0.2	0.9	0.2	1.8	0.4	0.8	0.3	0.7	0.2	0.9	0.4	9.9	2.4
Deep soils																						
Min	0.1	0.0	0.0	0.0	0.0	0.0	0.0	0.0	0.0	0.0	0.0	0.0	0.0	0.0	0.1	0.0	0.0	0.0	0.0	0.0	0.9	0.3
Max	4.3	1.5	25.7	3.5	59.0	7.0	15.5	2.4	5.0	1.2	11.5	2.1	87.2	20.4	4.2	1.6	3.6	1.3	9.0	3.4	171.7	33.2
Avg	0.6	0.2	1.1	0.2	1.4	0.2	0.9	0.1	0.9	0.2	0.7	0.1	1.6	0.4	0.8	0.3	0.7	0.3	0.9	0.3	9.7	2.3

Min, minimum; Max, maximum, Avg, average

[a]Based on conservative BTVs; [b]based on high BTVs

two horizons could be a reflection of pedogenetic/diagenetic control. While elements tend to move from higher to lower soil levels (Gregorauskienė and Kadūnas 2006), this does not seem to be the case in these soils. Higher median values for Zr, Hf, Ce, Th, U, and Sc (Fig. 3) in the deep soils likely reflect the preferential occurrence of these elements in minerals that have resistance to weathering. The elements typically associated with clay minerals and oxides/hydroxides (Fe, Al, Ti, V, and possibly Ga) are slightly accumulated in the deep soils (Fig. 3), probably reflecting their relationship with pedogenically formed Fe oxides. Conversely, Mn is a slightly enriched in the surface horizon and has a distinct behavior compared to Fe. These elements are both redox-sensitive and can leach from surface horizon under appropriate conditions and then re-precipitate in the underlying soil (Gregorauskienė and Kadūnas 2006). The distribution of Na and Mg is very similar between the two layers, whereas relatively lower concentrations of K, Ca, Ba, and Sr (Fig. 3) in the deep soils may be due to loss of more soluble elements during diagenesis/pedogenesis and the concomitant increase of refractory elements such as Al, Zr, and Hf. Median concentrations of Cd and P also show some variability, with higher concentrations in the surface soils that could be the result of different soil-forming processes or other factors. Similar median concentrations of As, Se, and Hg (Fig. 3) indicate a mainly natural control.

It is well known that anthropogenic activities can be cause of metal contamination which is typically concentrated in surface soils. On the other hand, there is some debate on whether the concentrations of elements in surface soil can be explained by the concentrations in the subsurface soil (Reimann and Garrett 2005). This study clearly indicates that, in the PSB, the surface soil geochemistry, to varying degree, can be related to deep soils concentrations and thus may contribute to surface concentrations and vice versa.

Recognition of geochemical signature and spatial patterns related to mineralization/bedrock lithology

The soils from the three major domains are clearly distinguished based on their geochemical characteristics based on LDA (Fig. 7b). This suggests the fact

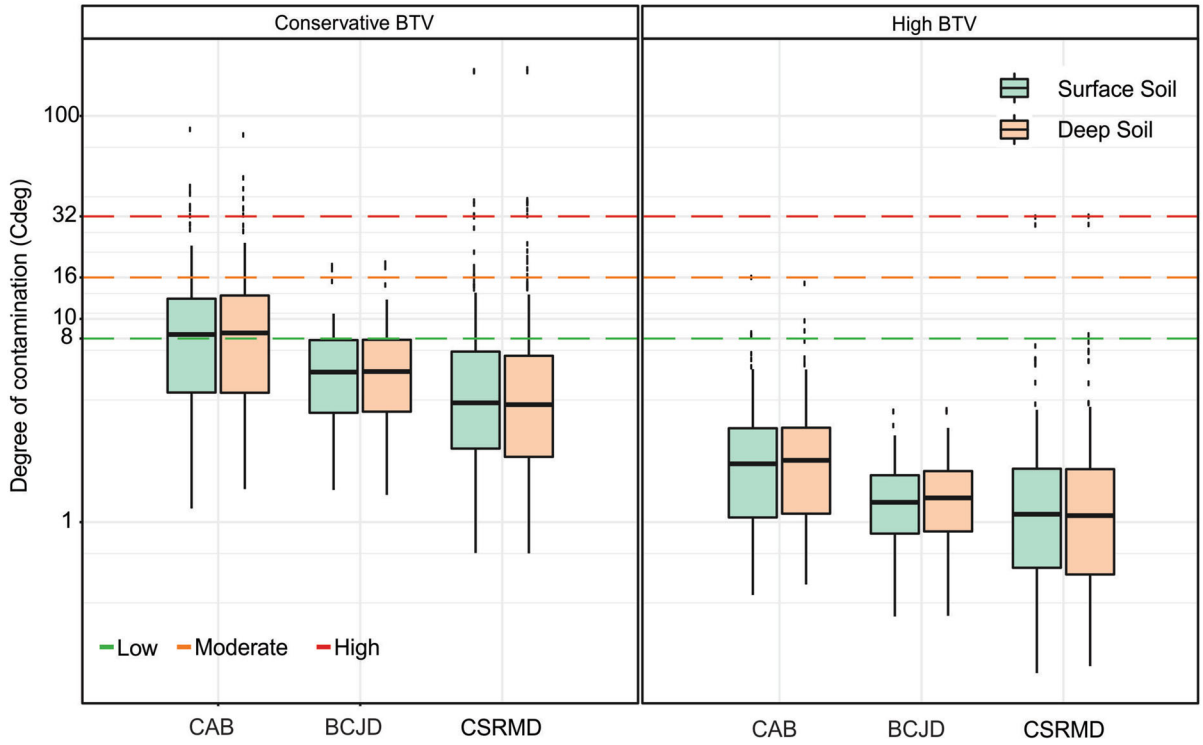

Fig. 8 Degree of contamination (C_{deg}) calculated for both surface and deep soils using the calculated 'conservative' and 'high' TBVs in different geologic settings of the PSB

that underlying lithology is the main factor controlling the surface soil geochemistry. In these cases, soil geochemistry is controlled by either physical/mechanical- or geochemical/biogeochemical-assisted vertical movement of elements from deeper to more shallow horizons (illuviation). Identifying specific geochemical signatures and the spatial pattern of group of samples that are representative of a particular deposit type/lithology also provides valuable information about the evolution of the underlying mineral deposits and gives evidence of the source and pathways of elements into the surface environment (Caritat et al. 2017; Sahoo et al. 2019). This was carried out using both log-transformed and clr-transformed multi-element data, and the results demonstrate a pronounced graphical contrast between log-transformed and clr-transformed data (Fig. 6). The closure effect is clearly distinct in the PCA result for the log-transformed data, while for the clr-transformed data the closure effect is eliminated and 'opens' or 'un-constrains' the data to reveal inherent correlations in the data that can provide straightforward interpretation (Filzmoser et al. 2009). The PCA groups variables into four principal clusters which may be interpreted in terms of geological setting, underlying lithology, mineralization, or other pedological and geochemical factors (Facchinelli et al. 2001; Burak et al. 2010). The Gp-1 (Fe–Ni–Cu–Cr–Sc–Ti–V) elemental association along with strong-to-moderate positive correlations between them is consistent with their similar geochemical behavior. It is certainly related to the local geological setting, mainly the metavolcanic rocks and BIFs concentrated in the Carajás basin and mafic and ultramafic units in other domains (Fig. 2), which made these elements available to soils as a result of supergene alteration (Ashley et al. 2012; Oze et al. 2004). Iron is grouped with V and Sc in Gp-1, has strong correlation, and shares a similar spatial distribution with both elements (Figs. 4, 6). These elements show higher concentrations in the soils of the Carajás basin and should be mainly related to banded-iron formations of the Carajás Formation, mafic metavolcanic rocks of the Parauapebas Formation, and lateritic crusts derived of supergenic alteration of diversified

units. The soils of the Canaã dos Carajás/Sapucaia/Rio Maria domains show lower concentration of Fe and V because granitoid rocks relatively impoverished in these elements are dominant in that geological setting (Figs. 2, 4). Moreover, under oxidizing conditions, Fe is concentrated as oxyhydroxides, which can co-precipitate trace elements, such as V, Ni, Cr, Cu (Burak et al. 2010; Hamon et al. 2004). Cu is linked with Fe, Ni, and Cr in Gp-1; however, its areal distribution is quite different than the other elements of this group. In fact, there is a close spatial correlation of Cu in soils with northern and southern copper belts that correspond to two independent zones of intense hydrothermal alteration which associated Cu-mineralization (Moreto et al. 2015). The Sossego copper mine and Cristalino copper deposit are situated in the southern belt. Copper is concentrated into sulfide minerals that are formed during hydrothermal alteration and are subsequently restricted to the sites of the hydrothermalized or altered rocks. Different kinds of rocks can host copper mineralization, such as metavolcanic rocks, gabbros, granitoids, which can be intensely affected by deformation and alteration along the hydrothermal corridor (Moreto et al. 2015; Monteiro et al. 2008). Furthermore, though Ni and Cr integrate the cluster Gp-1, they show different spatial distributions compared to Cu (Fig. 4) indicating that Cu enrichment in soils is not directly related to those of Ni and Cr. Strong positive correlation between Cr and Ni and their similar spatial distribution pattern can be explained by their geochemical affinity with mafic and ultramafic rocks (Ashley et al. 2012; Oze et al. 2004). Thus, soils developed from Parauapebas Formation in the Carajás basin, Sapucaia greenstone belt, and Vermelho mafic–ultramafic complex in the domains of southern PSB are enriched in Cr and Ni, while the lowest concentrations of these two elements in soils are associated with less mafic and granitoid rocks. High enrichment of these elements was also observed in the Vermelho sub-basin associated with mafic–ultramafic complexes of the Araguaia belt (Salomão et al. 2018).

Manganese is commonly associated with Fe, but in the soils of PSB it shows a different behavior than Fe. This possibly reflects different environmental conditions during pedogenetic process. An analogous situation was observed in surficial waters of the Vermelho and Sororó sub-basins of the Itacaiúnas watershed (cf. Salomão et al. 2018). Nevertheless, Mn is associated with Co, Pb, Zn, and Cd in Gp-4 and moderate-to-strong positive correlations between them are registered (Fig. 4). This may be attributed to the precipitation of Mn-oxyhydroxides with consequent adsorption and co-precipitation effect. Although, Pb and Zn can be associated with hydrothermalized rocks containing sulfides (e.g., galene and sphalerite), their poor correlation with S and the scarce occurrences of these sulfides in the PSB indicate that they could have come from other mineral sources.

The high positive loading of high field strength elements (HFSE), such as Zr, Hf, Nb, Y, along with Al, P, and Mo, in Gp-2 (Fig. 6) indicates that these elements could be associated with heavy mineral fractions in the matrix of clays and other silicate minerals. The HFSEs are mainly enriched in soils developed on felsic igneous rocks such as A-type Neoarchean and Paleoproterozoic granites (Salomão et al. 2018; Dall'Agnol et al. 2005, 2017). Mo is preferentially associated with calc-alkaline granites that occur near Água Azul do Norte (Salomão et al. 2018, and references therein) and Canaã dos Carajás (Feio et al. 2012). Furthermore, these elements are regarded as typical lithogenic elements that have very low mobility in the soil environment. This makes anthropogenic addition of these elements virtually absent, implying that their contents in the soil are a reflection of parent lithology (Souza et al. 2019; Fritsch et al. 2002).

Aluminum and LOI show strong correlation that can be probably attributed to formation of organic-rich clays which are an indicator of the natural process of soil formation. In general, the potentially toxic metals are adsorbed or chemisorbed into the Al-oxides or soil organic matter phases. However, the poor correlation between the potential toxic elements and Al and LOI indicates that the PTEs were already scavenged by other detrital minerals or different environmental conditions which did not favor their adsorption.

The alkaline and alkaline-earth elements such as K, Ca, Mg, Sr, Ba, and Rb are clustered in Gp-3. These elements are major constituents of common silicate minerals, and the positive correlation between these elements indicates influence in soils of aluminosilicate minerals, mainly feldspars and micas (Acosta et al. 2011; Towett et al. 2015). The mono/divalent elements, Na, Ca, and K, are highly mobile (Acosta et al. 2011). So, their low concentrations could be due to leaching in well-drained soils over long periods of

pedogenic weathering (Towett et al. 2015; Acosta et al. 2011). Typically, soils with high levels of Al and Fe contents, which is the case here, are depleted in the mobile elements and would account for why these elements are negatively correlated with major detritic elements such as Fe, Al, and Zr in the PCA results (Fig. 6). Furthermore, the spacial distribution of Ba and the areas with soils enriched in it (Fig. 4) appear to be linked to the dominance of Archean granitoids and gneisses, observed in the Canaã dos Carajás, Sapucaia, and Rio Maria domains. These geochemical associations and their spatial distribution in soils of PSB are similar between surface and deep samples, which strongly suggests a geogenic origin.

Determination of background threshold values

By definition, the background threshold value (BTV) is defined as the upper limit of background variation of a certain element in soil, which, theoretically, is free of anthropogenic influence (Reimann et al. 2005). Values above the threshold limit are present anomalous concentrations, which may be indicative of contamination, and further studies could be required concerning the local lithological and pedological characteristics and nearby anthropogenic activities in order to achieve solid conclusions about the origin of the high concentration values (Reimann et al. 2018). This study establishes the background levels of 18 elements, including potential toxic elements, which can be used to assess soil contamination in the study sites.

Although spatial distribution maps (Fig. 4) and statistical results (Table 2) demonstrate a close correspondence between the composition of surface soil (SS) and deep soils (DS), considering the environmental relevance of soils of two different horizons, their background threshold values were calculated separately. The results show that the BTVs of most of the elements between SS and DS are closely related. This clearly indicates that the elemental composition of surface soils is strongly influenced by local geology.

On the other hand, the different statistical methods had given values that varied significantly (Table 2), but each method has some unique characteristics. Thus, it is relevant to examine how the characteristics of each method will exert influence on the definition of geochemical background.

In the Brazilian Regulation listed in Resolution 420 (CONAMA 2009), the 75th percentile is one of the approaches that has been recommended for the estimation of 'quality reference values' (QRVs) for heavy metals and other substances in soils. In the present study, this approach gives the lowest threshold values and most of these values were below the PV limit as established by Resolution No. 420 of CONAMA (2009). Since this technique results in very restrictive or conservative estimates, the 75th percentile is defined as conservative (low) BTV (Table 2). This conservative limit can be an indication of pristine or natural conditions and can be useful from the perspective of protection of the environment or human health by identifying the sites posing a risk. However, using this method were identified a large number of sites that present anomalous values that will require attention or further investigation. This may sometimes be counterproductive and costly compared to taking into account only the few sites that may really present a problem. In addition, the low threshold values estimated by this method can reflect the unmineralized characteristics of an area. However, the Parauapebas basin is a typical mineralized area with active mines of iron and copper and associated deposits. Besides, it has a diversified geologic setting in which some specific lithologies may have higher contents of some elements compared to the normal background level and those lithologies will have a great influence on the overall background concentrations. This aspect is mostly ignored in environmental legislation/regulation when background values are used to distinguish potentially contaminated regions from pristine areas (Reimann and de Caritat 2017).

Furthermore, the large contrasts in spatial distribution of element concentrations and their association with specific lithologies/mineralizations demonstrate the need for another background, named as 'high BTV', which can represent the so-called mineralized/normal background. Several methods can be used to define 'high BTV. The percentile-based approach, such as 95th or 98th percentile, is widely used for background estimation and can be one option for this, but it provides a fixed number of cases that are in greater need of attention (Reimann et al. 2018). The highest values obtained for the TIF method often coincide with a break in the CP distribution that can correspond to the upper threshold and give the major contributions related to the specific lithology/

minerogenic contribution, as well as it can identify anomalous sites that really need closer attention (Kelepertzis et al. 2012; Mimba et al. 2018; Reimann and de Caritat 2017; Salomão et al. 2018). However, in this study, depending on the data distribution, TIF does not indicate the presence of outliers for some elements and estimated BTVs that exceed the maximum values, for instance Fe, Ba, Cu, Mo, and V. Also, in a few cases the BTVs were very close to the maximum values, for example Co, Pb, and Mn. The next higher values were estimated by M_{MAD}, which is distinct from pristine or natural background and usually represents the ambient/environment/normal background typical of geogenic plus anthropogenic diffuse origins (Reimann and Garrett 2005; Reimann and de Caritat 2017; Ander et al. 2013). In this study, this method provides very consistent high threshold values with closure in between the 95th and $\geq$ 98th percentiles, although some sites still require further investigation. The M_{MAD} values also exceeded the PV limits (CONAMA 2009) for elements such as Cr, Co, Ni, and Cu; these elements (except Ni) along with Fe and Mn also exceeded the 98th percentiles that can represent the mineralized/normal background. Thus, M_{MAD} appears to be the most appropriate method to define high BTV, except for Ba and V, for which the Q98 value is more appropriate (cf. values in Table 2).

Comparison of soil background values of the present study with those defined in other Brazilian states or regions

This study compares the elemental background concentration of soil elements within the Parauapebas sub-basin (PSB) with several other Brazil sites (Table 3) using data from the 75th percentile, which is defined as the quality reference value (QRV) by CONAMA Resolution No. 420/2009. Most of the elemental background values for PSB soils vary significantly with the values reported in other regions of Brazil, but some elements are similar (Table 3). The Fe background concentration is lower in PSB than reported in other regions, but is similar to the value obtained in Pará state by Fernandes et al. (2018). The background values of Cu and Mn in PSB are mostly higher than those estimated for other regions. It was also observed that the background level of Cu is higher than the PV limit as established by Resolution No. 420 of CONAMA (2009). Both aspects are clear evidence of the exceptional richness of Cu and Mn in PSB soils reflecting the fact that the entire area is situated in a copper- and manganese-enriched region. In comparison with specific studies, Noronha soils were found to be most enriched with several metals. The elevated trace element concentrations of Fernando de Noronha soils are due to the volcanic parent material which seems to be the main factor governing the relatively high natural concentrations of trace elements (Fabrício Neta et al. 2018). Furthermore, the background values reported by Caires (2009) for most analyzed metals, except Cu, Hg, Mo, and Mn, in soils of Minas Gerais (MG) were higher than the background values estimated for the PSB soils (Table 3). Additionally, the background values of Ni, Pb, Cr, Cu, Mn found in PSB are also higher than the values reported by Paye et al. (2010) for soils of the state of Espírito Santo (ES), but are lower for As and similar for Co, Mo, and Zn. The comparatively lower natural concentration of heavy metals found in Espirito Santo soils is due to the source material (Precambrian crystalline rocks and Tertiary and Quaternary sediments) (Paye et al. 2010). A similar picture is observed when comparing PSB soils with the Paraíba soils because the latter are derived mostly of Precambrian crystalline rocks (CPRM 2002).

Compared with Amazon soils, the background values of PSB soils are higher in all elements except Fe and Cd than those reported in northern and southern Amazonia soils. The background threshold values estimated for soils of Pará state of northern Brazil in different geologic settings by Fernandes et al. (2018) are lower for most elements than their equivalent in PSB (Table 3), except for Fe and As (similar) and Cd and Hg (higher). The background value of Ba was very high in the Fernando de Noronha soils and exceeded the QRV for an industrial scenario (750 mg kg^{-1}) suggested by CONAMA (2009); these soils have a volcanic origin in the archipelago (Table 3).

The comparison between soil backgrounds in different regions of Brazil demonstrates that there is a need for legislation based on cases that should be considered exceptions, because they represent geochemical differences of natural origin, but are currently treated as anomalies. This is well exemplified by copper in the PSB. For example, Biondi et al. (2011) suggest that areas with elevated levels of Ba, but without anthropic activity, require a thorough examination to evaluate Ba mobility and

bioavailability, to evaluate more rigorously the potential risk of using those areas. Besides, the high background values of Cu estimated in the PSB, exceeding IV values for agricultural soil indicated by CONAMA (2009), are likely due to Cu-mineralization originating from hydrothermally altered rocks and concentrate along two copper belts. This constitutes a remarkable geologic feature of the PSB that justifies the peculiar anomalous Cu values in its soils and is not verified in other regions.

Therefore, the metal concentration found in some examples taken for comparison confirms that the source material has a considerable influence on the geochemical composition of the soils and those derived from crystalline and sedimentary rocks tend to present lower concentration of metals. Thus, it is always essential to establish the background in each specific site in order to draw conclusions in environmental contamination studies, since specific properties of the pedogenetic formation or environmental factors can substantially affect the mobility and availability of trace elements. The results confirm the importance of determining background concentrations locally. With the definition of the natural content of elements in the deep soil and the estimation of the geochemical background, one can evaluate the degree of contamination of topsoils. Furthermore, the comparison between the results of this study with those available in the literature demonstrates that the background values are significantly different from one site to other, mainly due to the local geological setting and lithological characteristics of each site. It shows how risky it is to adopt the results of studies produced in other regions or countries as representative of local background for metals. Thus, it is emphasized that studies on appropriate contamination levels in soils should be found by previous determination of the local geochemical background.

Application of site-specific background values for environmental risk assessment

Because of extreme heterogeneity in soil geochemistry (locally, regionally, nationally, and globally), locally/regionally derived geochemical background values of soil elements can be better used to inform policy related to legislation and guidelines for soil/-land use or to delineate geogenic versus anthropogenic impacts (Morton-Bermea et al. 2009; Salminen and Tarvainen 1997). The contamination indices (CF and C_{deg}) based on conservative BTVs show that Ba, Pb, V, and Fe are not significant contaminants unlike Cr, Cu, Ni, and Co; the contamination was highest in the Carajás basin and Canaã dos Carajás region, which are intensely mined and contain mineral deposits of Cu, Fe, and Ni associated with the metavolcanic rocks and BIF and mafic/ultramafic units. The contamination levels are very similar between surface and deep soils (Fig. 8), indicating that this effect is not influenced by anthropogenic activities, such as mining (e.g., Sossego mine) or land use and land cover change, which are common in this region. Rather is this is caused by the natural geological processes, including the presence of mineral deposits. Therefore, when calculated potential contamination levels using high BTVs (considered as weathering of parent rocks and/or mineralization), low contamination was observed, which is also similar between surface and deep soils. This indicates that although the 75th percentile gives warning signal of contamination, the use of this method as a single BTV for the entire region may cause overestimation of environmental pollution, particularly in area having mineral deposits, which generally contain high contents of metals with geogenic (natural) origin. Therefore, using the high BTV values in this study (or any area having mineral deposits) results in more accurate estimation of heavy metal contamination from anthropogenic activities. Under similar conditions, it is important to pay more attention to the sites impacted by significant geogenic sources of potential contamination, which could cause environmental problems in the future. Special attention should be given to the processes of elemental mobilization in soils such as illuviation and eluviation, since changing physical, hydrological, geochemical and biological conditions can result in significant movement and placement of soil elements either as dissolved or suspended species during pedogenesis and diagenesis; constant monitoring of soil and water quality is needed to record any change in the soils and water quality in contaminated sites.

Conclusions

A regional-scale geochemical background survey of soils from Parauapebas basin, Brazil, provides the following conclusions:

- The high-density geochemical mapping along with multivariate analysis such as PCA and LDA effectively evaluated the source and geochemical behavior of potentially toxic elements (PTE) in soils.
- The strong geochemical similarity between surface and deep soils indicates a dominant geogenic (or natural) origin of elements including the PTEs, mostly related to the local variability of the parent materials, with apparently less (or insignificant) influence from anthropogenic activities.
- Centered log-transformed PCA provides interpretation of the multi-element geochemical signature in soils attributed to underlying lithology; the Fe–Ti–V–Sc–Cu–Cr–Ni–V group is related to metavolcanics, BIFs, and mafic and ultramafic rocks; the Zr–Hf–U–Nb–Th–Al–P–Mo–Ga group is related to A-type Neoarchean granitic or Paleoproterozoic granites; and Si–K–Na–Ca–Mg–Ba–Sr group is influenced by aluminosilicate minerals, mainly feldspars, and micas, contained in granitoids and gneisses.
- The spatial distribution of Fe, Ni, Cr, V, and Cu and their high enrichment in the Carajás Province are largely controlled by underlying lithology and/or mineralization. The Cr-Ni distribution is mostly influenced by mafic and ultramafic rocks, while Cu distribution is related to two hydrothermally mineralized copper belts.
- The background threshold values (BTVs) for surface and deep soils were closely related, but difference between methods was noted. The '75th percentile' provides conservative BTVs, while the 'M_{MAD}' gives high BTVs, which are more realistic for presenting mineralized/normal background in the study area.
- Contamination indices (CF and C_{deg}; based on 75th percentile) show that the sites associated with Carajás basin have high contamination, mostly from Cu, Cr, and Ni; however, this contamination was consistent between the surface and deep soils further indicating a strong geogenic rather than anthropogenic contamination in the soils of PSB. This interpretation was supported by the results of CF based on high BTVs.
- This study suggests that the anthropogenic contamination in the PSB soils cannot be correctly evaluated by using a single conservative BTV and highlights the need for another upper threshold value, defined as high BTVs, for its effectiveness.

Acknowledgements This work is part of the Itacaiúnas Geochemical Mapping and Background Project, ItacGMBP, currently being undertaken at Instituto Tecnológico Vale (ITV), Belém, Brazil. This was supported by Vale (GABAN-DIFN); Conselho Nacional de Desenvolvimento Científico e Tecnológico (CNPq) [DTI scholarship to GNS (Proc. 380.418/2018-5); Grants to RD (proc. 306108/2014-3; Proc. 443247/2015-3); RSA 305.392/2014-0]; and CAPES (scholarship to GCM, Proc. 88887.160998/2017-00). The authors acknowledge two anonymous reviewers for their constructive comments and insights and Marcondes Lima da Costa, Luiz Roberto Guimarães Guilherme, Otavio Augusto Boni Licht, José Francisco da Fonseca Ramos e José Francisco Bêrredo for their scientific collaboration with the Background project.

References

Acosta, J. A., Martínez-Martínez, S., Faz, A., & Arocena, J. (2011). Accumulations of major and trace elements in particle size fractions of soils on eight different parent materials. *Geoderma, 161*(1–2), 30–42. https://doi.org/10.1016/j.geoderma.2010.12.001.

Aitchison, J. (1986). *The statistical analysis of compositional data*. London: Chapman and Hall.

Almeida Júnior, A. B., Nascimento, C. W. A., Biondi, C. M., Souza, A. P., & Barros, F. M. R. (2016). Background and reference values of metals in soils from Paraíba State. *Brazil. Revista Brasileira de Ciência do Solo*. https://doi.org/10.1590/18069657rbcs20150122.

Alvares, C. A., Stape, J. L., Sentelhas, P. C., de Moraes Gonçalves, J. L., & Sparovek, G. (2013). Köppen's climate classification map for Brazil. *Meteorologische Zeitschrift, 22*(6), 711–728. https://doi.org/10.1127/0941-2948/2013/0507.

Ander, E. L., Johnson, C. C., Cave, M. R., Palumbo-Roe, B., Nathanail, C. P., & Lark, R. M. (2013). Methodology for the determination of normal background concentrations of contaminants in English soil. *Science of the Total Environment, 454–455,* 604–618. https://doi.org/10.1016/j.scitotenv.2013.03.005.

Ashley, P., Craw, D., MacKenzie, D., Rombouts, M., & Reay, A. (2012). Mafic and ultramafic rocks, and platinum mineralisation potential, in the Longwood Range, Southland, New Zealand. *New Zealand Journal of Geology and Geophysics, 55*(1), 3–19. https://doi.org/10.1080/00288306.2011.623302.

Berrow, M. L., & Reaves, G. A. (1984). Background levels of trace elements in soils. In *Proceedings of the 1st international conference on environmental contamination*. CEP Consultants. Edinburgh, Scotland (pp. 333–340).

Biondi, C. M., Nascimento, C. W. A., Fabrício Neta, A. B., & Ribeiro, M. R. (2011). Teores de Fe, Mn, Zn, Cu, Ni e Co em solos de referência de Pernambuco. *Revista Brasileira de Ciência do Solo, 35*(3), 1057–1066.

Boim, A. G. F., Rodrigues, S. M., dos Santos-Araújo, S. N., Pereira, E., & Alleoni, L. R. F. (2018). Pedotransfer functions of potentially toxic elements in tropical soils cultivated with vegetable crops. *Environmental Science and Pollution Research, 25*(13), 12702–12712. https://doi.org/10.1007/s11356-018-1348-0.

Burak, D. L., Fontes, M. P. F., Santos, N. T., Monteiro, L. V. S., Martins, E. S., & Becquer, T. (2010). Geochemistry and spatial distribution of heavy metals in Oxisols in a mineralized region of the Brazilian Central Plateau. *Geoderma, 160*(2), 131–142. https://doi.org/10.1016/j.geoderma.2010.08.007.

Caires, S. M. (2009). *Determination of natural heavy metals contents in soils of Minas Gerais State to help definition of background contents*. Ph.D. dissertation, Universidade Federal de Viçosa, Viçosa **(in Portuguese)**.

Caritat, P., Main, P. T., Grunsky, E. C., & Mann, A. W. (2017). Recognition of geochemical footprints of mineral systems in the regolith at regional to continental scales. *Australian Journal of Earth Sciences, 64*(8), 1033–1043.

CETESB. (2005). *Environmental Agency of the State of Sao Paulo*. Report on Establishment of Guiding Values for Soils and Groundwater of the State of Sao Paulo, São Paulo, Brazil (p. 247) **(in Portuguese)**.

Chiprés, J. A., Salinas, J. C., Castro-Larragoitia, J., & Monroy, M. G. (2008). Geochemical mapping of major and trace elements in soils from the Altiplano Potosino, Mexico: A multi-scale comparison. *Geochemistry: Exploration, Environment, Analysis, 8*(3–4), 279–290. https://doi.org/10.1144/1467-7873/08-181.

CONAMA. (2009). *National Council for the Environment, Brazil*. Resolution n° 420/2009. http://www.mma.gov.br/port/conama/legiabre.cfm?codlegi=620. Accessed January 16, 2017 **(in Portuguese)**.

Companhia de Pesquisa de Recursos Minerais (CPRM). (2002). *Serviço Geológico do Brasil. Geologia e recursos minerais do Estado da Paraíba*. Recife: Serviço Geológico do Brasil.

Dall'Agnol, R., da Cunha, I. R. V., Guimarães, F. V., de Oliveira, D. C., Teixeira, M. F. B., Feio, G. R. L., et al. (2017). Mineralogy, geochemistry, and petrology of *Neoarchean ferroan* to magnesian granites of Carajás Province, Amazonian Craton: The origin of hydrated granites associated with charnockites. *Lithos, 277,* 3–32. https://doi.org/10.1016/j.lithos.2016.09.032.

Dall'Agnol, R., Teixeira, N. P., Rämö, O. T., Moura, C. A. V., Macambira, M. J. B., & de Oliveira, D. C. (2005). Petrogenesis of the Paleoproterozoic rapakivi A-type granites of the Archean Carajás metallogenic province, Brazil. *Lithos, 80*(1–4), 101–129. https://doi.org/10.1016/j.lithos.2004.03.058.

de Moraes, B. C., da Costa, J. M. N., da Costa, A. C. L., & Costa, M. H. (2005). Variação espacial e temporal da precipitação no Estado do Pará. *Acta Amazonica, 35*(2), 207–214. https://doi.org/10.1590/S0044-59672005000200010.

De Vivo, B., Lima, A., Albanese, S., & Cicchella, D. (2003). *Atlante geochimico-ambientale della regione Campania (Geochemical Environmental Atlas of Campania Region)*. Napoli: De Frede Editore.

De Vivo, B., Lima, A., & Siegel, F. R. (2004). *Geochimica ambientale. Metalli potenzialmente tossici*. Naples: Liguori Editore.

Deschenes, S., Setton, E., Demers, P. A., & Keller, P. C. (2013). Exploring the relationship between surface and subsurface soil concentrations of heavy metals using geographically weighted regression. *E3S Web of Conferences, 1,* 35007. https://doi.org/10.1051/e3sconf/20130135007.

Fabrício Neta, A. B. (2012). *Teores naturais de metais pesados em solos da ilha de Fernando de Noronha [Dissertation in Portuguese]*. Recife: Universidade Federal Rural de Pernambuco.

Fabrício Neta, A. B., do Nascimento, C. W. A., Biondi, C. M., van Straaten, P., & Bittar, S. M. B. (2018). Natural concentrations and reference values for trace elements in soils of a tropical volcanic archipelago. *Environmental Geochemistry and Health, 40*(1), 163–173. https://doi.org/10.1007/s10653-016-9890-5.

Facchinelli, A., Sacchi, E., & Mallen, L. (2001). Multivariate statistical and GIS-based approach to identify heavy metal sources in soils. *Environmental Pollution, 114,* 313–324.

Fadigas, F. S., Sobrinho, N. M. B. A., Anjos, L. H. C., & Mazur, N. (2010). Background contents of some trace elements in weathered soils from the Brazilian Northern region. *Scientia Agricola, 67,* 53–59.

Feio, G. R. L., Dall'Agnol, R., Dantas, E. L., Macambira, M. J. B., Gomes, A. C. B., Sardinha, A. S., et al. (2012). Geochemistry, geochronology, and origin of the Neoarchean Planalto Granite suite, Carajás, Amazonian craton: A-type or hydrated charnockitic granites? *Lithos, 151,* 57–73. https://doi.org/10.1016/j.lithos.2012.02.020.

Feio, G. R. L., Dall'Agnol, R., Dantas, E. L., Macambira, M. J. B., Santos, J. O. S., Althoff, F. J., et al. (2013). Archean granitoid magmatism in the Canaã dos Carajás area: Implications for crustal evolution of the Carajás province, Amazonian craton, Brazil. *Precambrian Research, 227,* 157–185. https://doi.org/10.1016/j.precamres.2012.04.007.

Fernandes, A. R., de Souza, E. S., de Souza Braz, A. M., Birani, S. M., & Alleoni, L. R. F. (2018). Quality reference values and background concentrations of potentially toxic elements in soils from the Eastern Amazon, Brazil. *Journal of Geochemical Exploration, 90,* 453–463.

Filzmoser, P., Hron, K., & Reimann, C. (2009). Principal component analysis for compositional data with outliers. *Environmetrics, 20,* 621–632.

Fritsch, E., Montes-Lauar, C. R., Boulet, R., Melfi, A. J., Balan, E., & Magat, P. (2002). Lateritic and redoximorphic features in a faulted landscape near Manaus, Brazil. *European Journal of Soil Science, 53*(2), 203–217. https://doi.org/10.1046/j.1351-0754.2002.00448.x.

Galuszka, A. (2007). Different approaches in using and understanding the term "Geochemical Background"—Practical implications for environmental studies. *Polish Journal of Environmental Studies, 16,* 389–395.

Gregorauskienė, V., & Kadūnas, V. (2006). Vertical distribution patterns of trace and major elements within soil profile in Lithuania. *Geological Quarterly, 50*(2), 229–237.

Grunsky, E. C. (2010). The interpretation of geochemical survey data. *Geochemistry: Exploration, Environment and Analysis, 10,* 27–74.

Hakanson, L. (1980). An ecological risk index for aquatic pollution control. A sedimentological approach. *Water Research, 14,* 975–1001.

Hamon, R. E., McLaughlin, M. J., Gilkes, R. J., Rate, A. W., Zarcinas, B., Robertson, A., et al. (2004). Geochemical indices allow estimation of heavy metal background concentrations in soils. *Global Biogeochemical Cycles*. https://doi.org/10.1029/2003gb002063.

Jiao, X., Teng, Y., Zhan, Y., Wu, J., & Lin, X. (2015). Soil heavy metal pollution and risk assessment in Shenyang Industrial District, Northeast China. *PLoS ONE, 10*(5), e0127736. https://doi.org/10.1371/journal.pone.0127736.

Kabata-Pendias, A., & Mukherjee, A. B. (2007). *Trace elements from soil to human*. Berlin: Springer. https://doi.org/10.1007/978-3-540-32714-1.

Kabata-Pendias, A., & Pendias, H. (1992). *Trace elements in soils and plants*. Boca Raton: CRC Press.

Kelepertzis, E., Argyraki, A., & Daftsis, E. (2012). Geochemical signature of surface water and stream sediments of a mineralized drainage basin at NE Chalkidiki, Greece: A pre-mining survey. *Journal of Geochemical Exploration, 114,* 70–81. https://doi.org/10.1016/j.gexplo.2011.12.006.

Lancianese, V., & Dinelli, E. (2015). Different spatial methods in regional geochemical mapping at high density sampling: An application on stream sediment of Romagna Apennines, Northern Italy. *Journal of Geochemical Exploration, 154,* 143–155. https://doi.org/10.1016/j.gexplo.2014.12.014.

Marandi, A., & Karro, E. (2008). Natural background levels and threshold values of monitored parameters in the Cambrian–Vendian groundwater body, Estonia. *Environmental Geology, 54*(6), 1217–1225. https://doi.org/10.1007/s00254-007-0904-6.

Maritz, H., Cloete, H. C. C. C., & Elsenbroek, J. H. (2010). Analysis of high density regional geochemical soil samples at the council for geoscience (South Africa): The importance of quality control measures. *Geostandards and Geoanalytical Research, 34*(3), 265–273. https://doi.org/10.1111/j.1751-908X.2010.00078.x.

Martinez-Lladó, X., Vilà, M., Martí, V., Rovira, M., Domènech, J. A., & de Pablo, J. (2008). Trace element distribution in topsoils in Catalonia: Background and reference values and relationship with regional geology. *Environmental Engineering Science, 25*(6), 863–878. https://doi.org/10.1089/ees.2007.0139.

Matschullat, J., Ottenstein, R., & Reimann, C. (2000). Geochemical background—Can we calculate it? *Environmental Geology, 39*(9), 990–1000. https://doi.org/10.1007/s002549900084.

Mimba, M. E., Ohba, T., Nguemhe Fils, S. C., Nforba, M. T., Numanami, N., Bafon, T. G., et al. (2018). Regional geochemical baseline concentration of potentially toxic trace metals in the mineralized Lom Basin, East Cameroon: A tool for contamination assessment. *Geochemical Transactions, 19*(1), 11. https://doi.org/10.1186/s12932-018-0056-5.

Monteiro, L. V. S., Xavier, R. P., Hitzman, M. W., Juliani, C., de Souza Filho, C. R., & Carvalho, E. R. (2008). Mineral chemistry of ore and hydrothermal alteration at the Sossego iron oxide–copper–gold deposit, Carajás Mineral Province, Brazil. *Ore Geology Reviews, 34*(3), 317–336. https://doi.org/10.1016/j.oregeorev.2008.01.003.

Moreto, C. P. N., Monteiro, L. V. S., Xavier, R. P., Creaser, R. A., DuFrane, S. A., Melo, G. H. C., et al. (2015). Timing of multiple hydrothermal events in the iron oxide–copper–gold deposits of the Southern Copper Belt, Carajás Province, Brazil. *Mineralium Deposita, 50,* 517–546.

Morton-Bermea, O., Hernández-Álvarez, E., González-Hernández, G., Romero, F., Lozano, R., & Beramendi-Orosco, L. E. (2009). Assessment of heavy metal pollution in urban topsoils from the metropolitan area of Mexico City. *Journal of Geochemical Exploration, 101*(3), 218–224. https://doi.org/10.1016/j.gexplo.2008.07.002.

Nakić, Z., Posavec, K., & Bačani, A. (2007). A visual basic spreadsheet macro for geochemical background analysis. *Ground Water, 45,* 642–647.

Nascimento, C. W. A., Lima, L. H. V., Silva, F. L. S., Biondi, C. M., & Campos, M. C. C. (2018). Natural concentrations and refernce values of heavy metals in sedimentary soils in the Brazilian Amazon. *Environmental Monitoring and Assessment*, *190*, 606. https://doi.org/10.1007/s10661-018-6989-4.

Ohta, A., Imai, N., Terashima, S., & Tachibana, Y. (2011). Regional geochemical mapping in eastern Japan including the nation's capital, Tokyo. *Geochemistry: Exploration, Environment, Analysis, 11*(3), 211–223. https://doi.org/10.1144/1467-7873/10-042.

Oze, C., Fendorf, S., Bird, D. K., & Coleman, R. G. (2004). Chromium geochemistry in serpentinized ultramafic rocks and serpentine soils from the Franciscan complex of California. *American Journal of Science, 304*(1), 67–101. https://doi.org/10.2475/ajs.304.1.67.

Palumbo, B., Angelone, M., Bellanca, A., Dazzi, C., Hauser, S., Neri, R., et al. (2000). Influence of inheritance and pedogenesis on heavy metal distribution in soils of Sicily, Italy. *Geoderma, 95*(3–4), 247–266. https://doi.org/10.1016/S0016-7061(99)00090-7.

Pandolfo, C. M., Ceretta, C. A., Massignam, A. M., da Veiga, M., & Moreira, I. C. L. (2008). Análise ambiental do uso de fontes de nutrientes associadas a sistemas de manejo do solo. *Revista Brasileira de Engenharia Agrícola e Ambiental, 12*(5), 512–519. https://doi.org/10.1590/S1415-43662008000500012.

Paye, H. S., de Mello, J. W. V., Abrahão, W. A. P., Fernandes Filho, E. I., Dias, L. C. P., Castro, M. L. O., et al. (2010). Valores de referência de qualidade para metais pesados em solos no Estado do Espírito Santo. *Revista Brasileira de Ciência do Solo, 34*(6), 2041–2051. https://doi.org/10.1590/s0100-06832010000600028.

Pontes, P. R. M., Cavalcante, R. B. L., Sahoo, P. K., Silva, R., Jr., Silva, M. S., Dall'Agnol, R., et al. (2019). The role of protected and deforested areas in the hydrological processes of Itacaiúnas River Basin, eastern Amazonia. *Journal of Enviromental Mangament, 235,* 489–499.

Preston, W., Nascimento, C. W. A., Biondi, C. M., Souza Junior, V. S., Silva, W. R., & Ferreira, H. A. (2014). Quality reference values for heavy metals in soils of Rio Grande do Norte, Brazil. *Revista Brasileira de Ciência do Solo, 38,*

1028–1037. https://doi.org/10.1590/S0100-06832014000300035. **(in Portuguese with English abstract)**.

R Core Team. (2018). *R: A language and environment for statistical computing*. R Foundation for Statistical Computing, Vienna. https://www.R-project.org. Accessed 21 Jan 2018.

Reimann, C., & de Caritat, P. (2017). Establishing geochemical background variation and threshold values for 59 elements in Australian surface soil. *Science of the Total Environment, 578,* 633–648. https://doi.org/10.1016/j.scitotenv.2016.11.010.

Reimann, C., Fabian, K., Birke, M., Filzmoser, P., Demetriades, A., Négrel, P., et al. (2018). GEMAS: Establishing geochemical background and threshold for 53 chemical elements in European agricultural soil. *Applied Geochemistry, 88,* 302–318. https://doi.org/10.1016/j.apgeochem.2017.01.021.

Reimann, C., Filzmoser, P., & Garrett, R. (2002). Factor analysis applied to regional geochemical data: Problems and possibilities. *Applied Geochemistry, 17*(3), 185–206. https://doi.org/10.1016/S0883-2927(01)00066-X.

Reimann, C., Filzmoser, P., & Garrett, R. G. (2005). Background and threshold: Critical comparison of methods of determination. *Science of the Total Environment, 346,* 1–16.

Reimann, C., & Garrett, R. G. (2005). Geochemical background—Concept and reality. *Science of the Total Environment, 350*(1–3), 12–27. https://doi.org/10.1016/j.scitotenv.2005.01.047.

Sahoo, P. K., Guimarães, J. T. F., Souza-Filho, P. W. M., Powell, M. A., Silva, M. S., Moraes, A. M., et al. (2019). Statistical analysis of lake sediment geochemical data for understanding surface geological factors and processes: An example from Amazonian upland lakes, Brazil. *CATENA, 175,* 47–62.

Salminen, R., & Tarvainen, T. (1997). The problem of defining geochemical baselines: A case study of selected elements and geological materials in Finland. *Journal of Geochemical Exploration, 60*(1), 91–98. https://doi.org/10.1016/s0375-6742(97)00028-9.

Salomão, G. N., Dall'Agnol, R., Sahoo, P. K., Júnior, J. S. F., Silva, M. S., Souza Filho, P. W., et al. (2018). Geochemical distribution and thresholds values determination of heavy metals in stream water in the sub-basins of Vermelho and Sororó rivers, Itacaiúnas River watershed, Eastern Amazon, Brazil. *Geochimica Brasiliensis*, *32*, 179–197.

Santos, S. N., & Alleoni, L. R. F. (2013). Reference values for heavy metals in soils of Brazilian agricultural frontier in Southwestern Amazônia. *Environmental Monitoring and Assessment, 185,* 5737–5748.

Schober, P., Boer, C., & Schwarte, L. A. (2018). Correlation coefficients: Appropriate use and interpretation. *Anesthesia and Analgesia, 126,* 1763–1768. https://doi.org/10.1213/ANE.0000000000002864.

Silva, Y. J., Nascimento, C. W., Cantalice, J. R., da Silva, Y. J., & Cruz, C. M. (2015). Watershed-scale assessment of background concentrations and guidance values for heavy metals in soils from a semiarid and coastal zone of Brazil. *Environmental Monitoring and Assessment*, *187*(9), 558. https://doi.org/10.1007/s10661-015-4782-1.

Souza, J. J. L. L., Fontes, M. P. F., Gilkes, R., da Costa, L. M., & de Oliveira, T. S. (2019). Geochemical signature of Amazon tropical rainforest soils. *Revista Brasileira de Ciencia do Solo, 42,* 1–18. https://doi.org/10.1590/18069657rbcs20170192.

Souza-Filho, P. W. M., Souza, E. B., Silva Júnior, R. O., Nascimento, W. R., Jr., Mendonça, B. R. V., Guimarães, J. T. F., et al. (2016). Four decades of land-cover, land-use and hydroclimatology changes in the Itacaiúnas River watershed, southeastern Amazon. *Journal of Environmental Management, 167,* 175–184. https://doi.org/10.1016/j.jenvman.2015.11.039.

Teh, T., Norulaini, N. A. R., Shahadat, M., Wong, Y., & Mohd Omar, A. K. (2016). Risk assessment of metal contamination in soil and groundwater in Asia: A review of recent trends as well as existing environmental laws and regulations. *Pedosphere, 26*(4), 431–450. https://doi.org/10.1016/S1002-0160(15)60055-8.

Teixeira, M. F. B., Dall'Agnol, R., Santos, J. O. S., de Sousa, L. A. M., & Lafon, J.-M. (2017). Geochemistry, geochronology and Nd isotopes of the Gogó da Onça Granite: A new Paleoproterozoic A-type granite of Carajás Province, Brazil. *Journal of South American Earth Sciences, 80,* 47–65. https://doi.org/10.1016/j.jsames.2017.09.017.

Thornton, I., Farago, M. E., Thums, C. R., Parrish, R. R., McGill, R. A. R., Breward, N., et al. (2008). Urban geochemistry: Research strategies to assist risk assessment and remediation of brownfield sites in urban areas. *Environmental Geochemistry and Health, 30*(6), 565–576. https://doi.org/10.1007/s10653-008-9182-9.

Towett, E. K., Shepherd, K. D., Tondoh, J. E., Winowiecki, L. A., Lulseged, T., Nyambura, M., et al. (2015). Total elemental composition of soils in Sub-Saharan Africa and relationship with soil forming factors. *Geoderma Regional, 5,* 157–168. https://doi.org/10.1016/j.geodrs.2015.06.002.

Vasquez, L. V., Rosa-Costa, L. R., Silva, C. G., Ricci, P. F., Barbosa, J. O., & Klein, E. L. (2008). *Geologia e recursos minerais do estado do Pará: Sistema de Informações Geográficas – SIG: Texto explicativo dos mapas geológico e tectônico e de recursos minerais do estado do Pará*. http://rigeo.cprm.gov.br/jspui/handle/doc/10443.

Wang, Z., Hong, C., Xing, Y., Wang, K., Li, Y., Feng, L., et al. (2018). Spatial distribution and sources of heavy metals in natural pasture soil around copper-molybdenum mine in Northeast China. *Ecotoxicology and Environmental Safety, 154,* 329–336. https://doi.org/10.1016/j.ecoenv.2018.02.048.

Xie, X., Wang, X., Zhang, Q., Zhou, G., Cheng, H., Liu, D., et al. (2008). Multi-scale geochemical mapping in China. *Geochemistry: Exploration, Environment, Analysis, 8*(3–4), 333–341. https://doi.org/10.1144/1467-7873/08-184.

Yamamoto, K., Tanaka, T., Minami, M., Mimura, K., Asahara, Y., Yoshida, H., et al. (2007). Geochemical mapping in Aichi prefecture, Japan: Its significance as a useful dataset for geological mapping. *Applied Geochemistry, 22*(2), 306–319. https://doi.org/10.1016/j.apgeochem.2006.09.011.

Zuo, R. (2011). Identifying geochemical anomalies associated with Cu and Pb–Zn skarn mineralization using principal component analysis and spectrum–area fractal modeling in the Gangdese Belt, Tibet (China). *Journal of Geochemical*

Exploration, 111(1–2), 13–22. https://doi.org/10.1016/j.gexplo.2011.06.012.

Zuo, R., Cheng, Q., Agterberg, F. P., & Xia, Q. (2009). Application of singularity mapping technique to identify local anomalies using stream sediment geochemical data, a case study from Gangdese, Tibet, western China. *Journal of Geochemical Exploration, 101*(3), 225–235. https://doi.org/10.1016/j.gexplo.2008.08.003.